Quaternary International 258 (2012) 148–164

Contents lists available at SciVerse ScienceDirect

Quaternary International

journal homepage: www.elsevier.com/locate/quaint

A southern Indian Middle Palaeolithic occupation surface sealed by the 74 ka Toba eruption: Further evidence from Jwalapuram Locality 22

Michael Haslam[a,*], Chris Clarkson[b], Richard G. Roberts[c], Janardhana Bora[d], Ravi Korisettar[d], Peter Ditchfield[a], Allan R. Chivas[c], Clair Harris[b], Victoria Smith[a], Anna Oh[a], Sanjay Eksambekar[e], Nicole Boivin[a], Michael Petraglia[a]

[a] Research Laboratory for Archaeology and the History of Art, School of Archaeology, University of Oxford, Dyson Perrins Building, South Parks Road, Oxford OX1 3QY, United Kingdom
[b] School of Social Science, University of Queensland, St Lucia, QLD 4072, Australia
[c] Centre for Archaeological Science, School of Earth & Environmental Science, University of Wollongong, Wollongong, NSW 2522, Australia
[d] Department of History and Archaeology, Karnatak University, Dharwad 580 003, India
[e] Phytolith Research Institute, 3, Pragati, Near Kakade Park, Chinchwad, Pune 411 033, India

ARTICLE INFO

Article history:
Available online 10 September 2011

ABSTRACT

This paper reports further evidence from an archaeological occupation surface in southern India that was buried by tephra from the Toba volcanic super-eruption ca. 74,000 years ago. The open-air site, designated Jwalapuram Locality 22 and located in the Kurnool District of Andhra Pradesh, preserves more than 1600 stone artefacts assigned to the Indian Middle Palaeolithic. Sedimentological, isotopic and lithic data along with optically stimulated luminescence ages confirm the site as occupied closely prior to the eruption. The hominin taxon responsible for creating the site is not known, but the stone tool evidence is most consistent with contemporaneous *Homo sapiens* technologies in Africa and to the east of South Asia. The findings have relevance for understanding Indian Middle Palaeolithic technology, and for identifying the behavioural and environmental adaptations of the hominin group(s) that occupied India when Toba erupted.

1. Introduction

South Asia preserves a record of hominin occupation extending back into the Early Pleistocene (Dennell, 2007, 2009; Pappu et al., 2011). The regional Middle and Late Pleistocene lithic record can be broadly divided into Acheulean, Middle Palaeolithic and microlithic industries (Settar and Korisettar, 2002), and recent analyses have increased knowledge of the technological, environmental and behavioural contexts of the Acheulean and microlithic phases in particular (Petraglia, 1998, 2006; Pappu, 2002; Clarkson et al., 2009; Kourampas et al., 2009; Petraglia et al., 2009a; Perera, 2010; Haslam et al., 2011; Pappu et al., 2011; Perera et al., 2011). However, despite its relatively widespread recognition throughout the region (Pal, 2002), the South Asian Middle Palaeolithic has received comparatively less attention. Ages for this industry remain somewhat sparse and problematic, but likely fall within Marine Isotope Stages (MIS) 5 to 3 (Misra, 1989; Achyuthan et al., 2007; Petraglia et al., 2009b), which importantly likely encompasses the period of early *Homo sapiens* dispersals eastwards out of Africa (Mellars, 2006; Oppenheimer, 2009; Petraglia et al., 2010).

The Indian Middle Palaeolithic is characterised by the manufacture from cryptocrystalline cores (including discoidal and Levallois techniques) of a variety of flake tools such as scrapers and points (Sankalia, 1964; Pal, 2002). The early stages of this phase have been viewed as overlapping with and perhaps developing out of the South Asian Late Acheulean industry (Mishra, 1995), based on assemblages that contain a proportion of refined diminutive handaxes (Haslam et al., in this volume; Haslam et al., 2011). The eruption of the Sumatran Toba super-volcano around 74 ka has also assumed increasing importance in recent Indian Late Pleistocene studies, both for providing an isochronous Youngest Toba Tuff (YTT) marker across India and as a potential driver of severe climatic deterioration close to the posited time of human dispersal (Rampino and Self, 1992, 1993; Acharyya and Basu, 1993; Westgate et al., 1998; Rampino and Ambrose, 2000; Jones and Pal, 2005; Jones, 2007, 2010; Robock et al., 2009; Williams et al., 2009, 2010; Haslam and Petraglia, 2010). Recent data suggest that climatic upheaval caused by the eruption was not as severe as first hypothesised, as previous sulphur outputs from the caldera were likely vastly over-estimated

* Corresponding author.
E-mail address: michael.haslam@rlaha.ox.ac.uk (M. Haslam).

1040-6182/$ – see front matter © 2011 Elsevier Ltd and INQUA. All rights reserved.
doi:10.1016/j.quaint.2011.08.040

(Chesner and Luhr, 2010; Oppenheimer, 2011). Nevertheless, a key focus for current research is the taxonomic identity and behavioural adaptations of South Asian Middle Palaeolithic hominins at the time of the eruption.

The authors recently reported initial findings from Jwalapuram Locality 22, an occupation surface sealed by a YTT layer in the Jurreru Valley of southern India (Haslam et al., 2010a). While other finds from this valley have previously been constrained by chronometric dates to within several thousand years prior to the eruption (Haslam et al., 2010b), other than at Jwalapuram Locality 22 a direct association has not been observed between the YTT and archaeological remains. This paper expands upon the initial report of this site through sedimentological, palaeoenvironmental and lithic technological analyses, providing a new perspective on the human populations that witnessed the Toba ash-fall. Discussion in this paper is primarily concerned with the finds and contexts below the YTT deposits at Locality 22.

2. Jwalapuram Locality 22

Jwalapuram Locality 22 (15°19'23.9"N, 8°07'48.5"E; Fig. 1) is located topographically at a point where the Jurreru Valley opens from a relatively constricted course (cut through the Erramalai Hills, a component of the Eastern Ghats) to a wider alluvial plain. The Locality 22 site sits on the western margin of a localised shallow basin, which held a wetland component when Toba erupted and was in-filled by extensive wind-blown and sheetwash YTT ash deposits in the subsequent years (Jones, 2010; Matthews et al., 2012). The site was discovered by tracing exposures of the buried YTT layer across the landscape away from its thickest accumulation of over 2.5 m, to where the ash pinches out and the deposition of the primary tephra was most likely sub-aerial. These conditions mark the intersection of higher, dry terrain with the wetlands, a zone that would have attracted both resident hominins and prey species. The initial hypothesis was, therefore, that the buried Locality 22 surface was exposed and vegetated at the time of the tephra-fall in the valley. This stands in contrast to Jwalapuram Locality 3, some 400 m to the east, which was situated in a topographical low and where more than 1 m of clays was deposited between the time of occupation and the primary ash-fall (Blinkhorn et al., 2012; Petraglia et al., 2007; Haslam et al., 2010b).

Locality 22 preserves a tephra layer approximately 2 m below the present, flat ground surface (Fig. 2a; Fig. 3). Beneath a thin, disturbed modern topsoil layer lie approximately 1.8–2 m of reddish yellow silts (thickening towards the south), with some sediment texture variation but no colour changes and numerous large calcareous

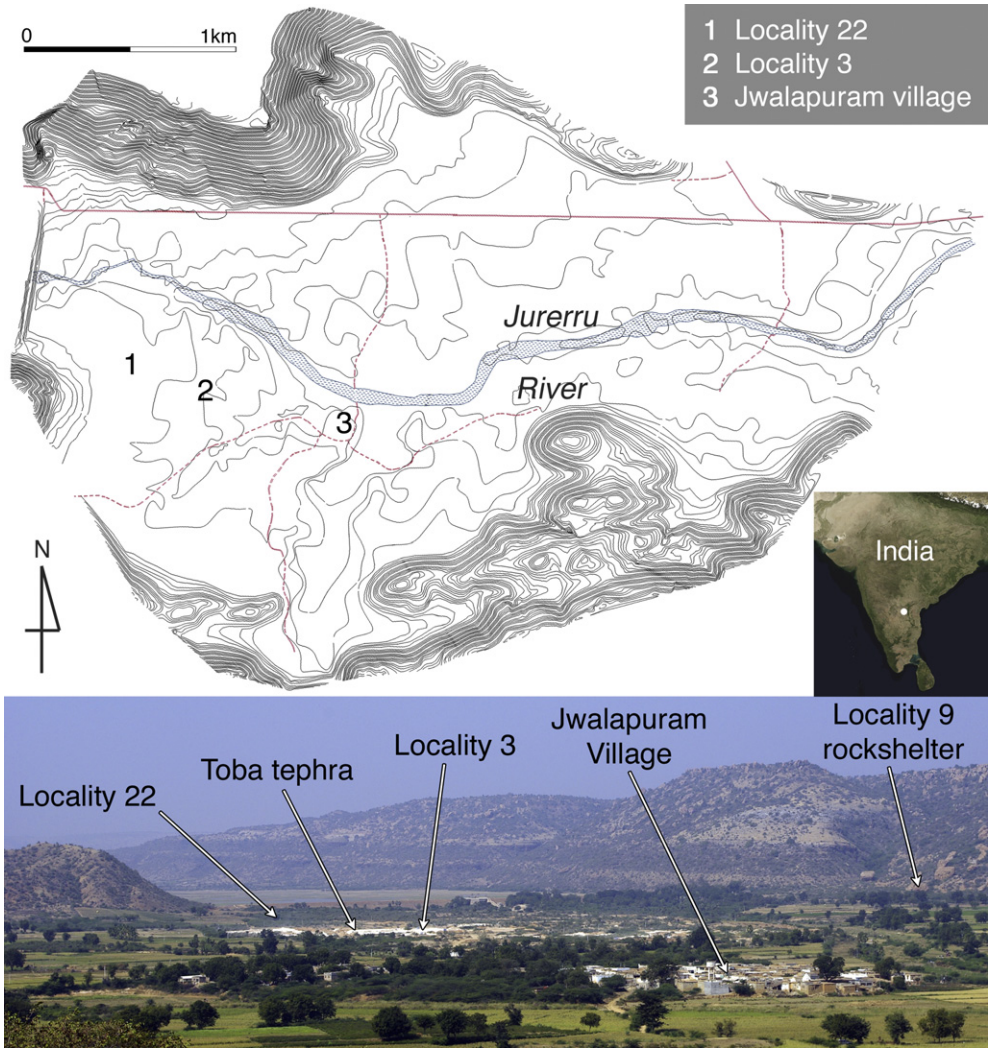

Fig. 1. Map (2 m contours) and photograph (facing northwest) showing the location of Jwalapuram Locality 22, Jurreru River Valley. Nearby sites and landscape features are indicated. Inset shows position of Jurreru Valley in southern India.

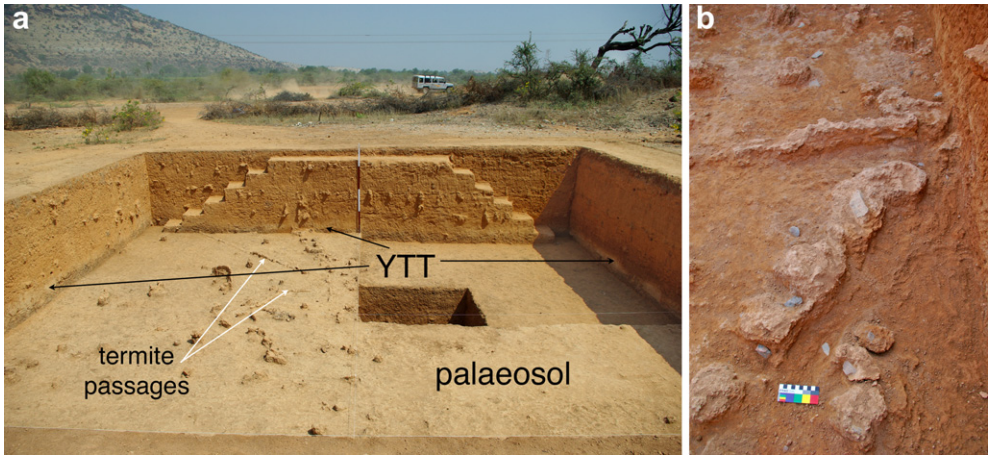

Fig. 2. (a) Jwalapuram Locality 22 during excavation, with the palaeosol (darker sediment at base of each profile) exposed, and indicating the position of the overlying YTT layer. Facing northeast; the scale has 50 cm intervals; (b) Limestone artefacts and calcareous concretions in situ at the YTT-palaeosol interface; scale is in cm.

nodules derived from groundwater fluctuations. This thick bed is culturally sterile except for a small number of stone artefacts, including a microblade core, in slightly coarser, mineral-rich sediment 1.5–1.8 m below the surface. Optically stimulated luminescence (OSL) dating of the sediments above the tephra at Locality 22 and other excavated sites in the Jurreru Valley suggest a local sedimentation gap of c. 35,000 years following the Toba event (Balter, 2010; Roberts et al., 2010), contrary to initial reports (Petraglia et al., 2012; Petraglia et al., 2007). The microblade core at Locality 22 supports this suggestion, as microblades do not become common in the Jurreru Valley until 38–35 ka (Clarkson et al., 2012). Below the mineral-rich layer, the lower 20–30 cm of the reddish yellow silts has an increasing tephra content, culminating in unmixed pods of tephra forming an undulating but sharp contact with a yellowish brown palaeosol at around 1.9–2 m depth (this interface is higher towards the north). The upper interface of the palaeosol preserves abundant lithic artefacts (Fig. 2b), as well as termite nests and passageways preserved as micritic carbonate structures. With increasing depth below the interface, sediments become darker and contain lenses of coarser material (just below 4 m and 6 m depth) in a very fine sand matrix.

Locality 22 was excavated over two seasons (2008–09), initially as a 5 × 5 m trench and later as an expanded 10 × 10 m excavation (the excavated area at the tephra–palaeosol interface was reduced to 22.75 m^2 and 95.5 m^2 in the respective seasons by leaving a set of access steps extending from the site's north-eastern wall). The trench is oriented at 45° west of magnetic north, with grid north aligned to the northwest. All excavation was by hand using trowels, chisels and small picks, with sediments sieved through 5 mm mesh screens. Artefacts were piece-plotted in situ in three dimensions using either manual mapping or a total station. Fortunately, and unlike the majority of land in the Jurreru Valley, Locality 22 had not previously been targeted by local villagers for either ash quarrying or agricultural production. However, with the accelerating rate of such activities it appears inevitable that this will occur within the next few decades. Excavation ceased in both field seasons upon reaching the local water table at depths of ~3.5 m (2008 season) and ~6.4 m (2009 season).

3. Age of the Locality 22 sediments

Four sediment samples were collected from below the YTT for OSL dating (Fig. 3). Metal tubes were hammered into the cleaned section faces at depths of 216 cm (J22/4), 371 cm (J22/5), 512 cm (J22-2009/2) and 612 cm (J22-2009/1), and then sealed in black plastic bags after removal. Three sediment samples were also taken from above the YTT layer (J22/1, J22/2 and J22/3; Fig. 3), but as they date to ca. 40 ka (Roberts et al., 2010) these samples are not discussed here. A full report on these and other OSL ages is forthcoming.

OSL dating provides an estimate of the time since grains of quartz or feldspar were last exposed to sunlight (Huntley et al., 1985; Aitken, 1998). Ultraviolet OSL emissions from individual sand-sized grains of quartz were measured to benefit from the advantages of single-grain OSL dating (Jacobs and Roberts, 2007). The burial age of a grain is determined by dividing the equivalent dose (D_e), which is estimated by measuring the OSL signal, by the environmental dose rate due mainly to the radioactive decay of ^{238}U, ^{235}U, ^{232}Th (and their daughters) and ^{40}K in the surrounding deposit. (See the supplementary online material (SOM) for further details of the OSL methods).

Table 1 lists the burial ages of the four OSL samples, as well as the supporting data for the dose rates and D_e estimates. To determine these ages, between 500 and 1000 individual grains of each sample were measured, resulting in between 149 and 289 independent estimates of D_e from those grains that passed all of the single-aliquot regenerative-dose (SAR) performance criteria (SOM; Table 1). Around half of the grains in each sample (43–50%) were rejected because their test-dose OSL signals were indistinguishable from background. The 19–29% of grains used for D_e determination were characterised by a rapid decay of OSL with stimulation (indicative of them being dominated by the 'fast' component of quartz OSL, which is a requirement for the reliable application of the SAR procedure) and by the continued growth of the OSL signal at high doses (which allowed large D_e values to be measured). Petraglia et al. (2007) shows OSL decay and dose–response curves for three individual grains from Locality 3, which are representative also of the behaviours of the accepted grains from Locality 22.

The D_e distributions of all four samples have 'overdispersion' (OD) values of 22–35% (Table 1). These represent the relative scatter in D_e remaining after taking measurement uncertainties into account (Galbraith et al., 1999), and are similar to the OD values of 26–28% obtained for the single-grain D_e distributions at Localities 3 and 21 (2009a; 2009b; Petraglia et al., 2007). They are slightly higher, however, than those commonly reported for well-bleached samples that have not been affected after deposition by sediment mixing or spatial heterogeneity in the dose rate (Jacobs and Roberts, 2007; Arnold and Roberts, 2009). The measured D_e values are displayed as radial plots in Fig. 4. Each point represents the D_e value for a single grain, which can be read by drawing a line from the origin of the 'standardized estimate' axis, through the point of interest, until it

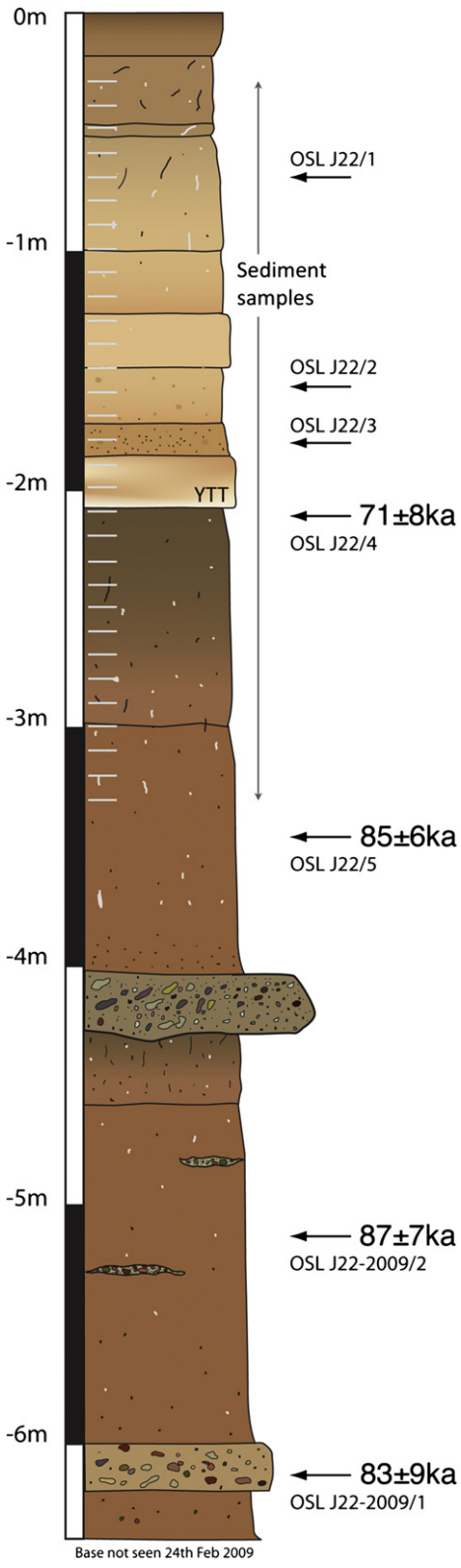

Fig. 3. Sediment log showing position of analysed sediment samples (white bars at 30–330 cm depth, with SS1 uppermost and SS31 lowermost) and OSL samples (arrowed), southeast profile, Jwalapuram Locality 22.

intersects the D_e axis. The uncertainty on this D_e is obtained by drawing a vertical line from the data point to intersect the 'relative error' axis. D_e values measured with the greatest precision fall furthest to the right, and any shaded band of ± 2 units projecting from the standardised estimate axis will capture 95% of the points if they are statistically consistent (Galbraith et al., 1999). All four samples have similar D_e distributions, but it is apparent that no single shaded band can accommodate all D_e estimates for any of the samples. In each case, many values are less than the D_e used to estimate the OSL age, which is indicated by the shaded band in Fig. 4. The D_e value of the latter 'main component', which contains the majority of grains (53–83%, Table 1), was obtained using the Finite Mixture Model (Roberts et al., 2000), together with formal statistical criteria to determine the fewest D_e components required to fit the measured D_e distributions (David et al., 2007; Jacobs et al., 2008b). Two- or three-component fits with an OD of 15% or 10%, respectively, were sufficient to accommodate the observed scatter in D_e for these four samples.

D_e values smaller than the main component are attributed to these grains being located next to, or encased by, carbonates, which have negligible radioactivity and will, therefore, expose the adjacent grains to greatly reduced beta dose rates (Turney et al., 2008; Jacobs et al., 2008a, 2008b; Haslam et al., 2011). A similar explanation was offered for the overdispersed single-grain D_e distribution of the OSL sample collected from beneath the YTT at Locality 3 (Petraglia et al., 2007). Soil carbonate is variably present in sediments above and below the YTT at Jwalapuram (Jones, 2010). To estimate the beta dose rate experienced by the grains in the main D_e component of each sample, the procedure described in Jacobs et al. (2008c) and Haslam et al. (2011), which also provide worked examples, was used. The total dose rate for each sample was then calculated using the adjusted beta dose rate, which is shown alongside the original (uncorrected) value in Table 1. This procedure is only valid if the age calculated for the population of grains with the smallest D_e values, when divided by the total dose rate with the beta contribution set to zero (to mimic grains surrounded entirely by carbonate), equals or exceeds that determined for grains in the main component (with the D_e divided by the total dose rate including the beta contribution). All four samples satisfied this requirement, from which it is inferred that all grains in a particular sample had been deposited at the same time, but had subsequently experienced a range of beta dose rates. Any changes in dose rate due to carbonate cementation over the period of sample burial (Nathan and Mauz, 2008) are minimised using this approach, as the OSL ages are estimated for the grains surrounded mostly or entirely by non-carbonate materials.

Some other causes of low D_e values can be discounted, such as contamination by feldspar, which is well known to produce age shortfalls; such grains (81 of the 3200 measured) had been identified and rejected already using the SAR performance criteria. Post-depositional sediment mixing can introduce younger grains from overlying deposits, and these would likely have smaller D_e values. In particular, sample J22/4 is located only 10 cm below the YTT/palaeosol interface and could potentially have been bioturbated by termite activity. As discussed in Section 4 below, however, the absence of tephra in the underlying palaeosol, and the lack of artefact movement upwards into the YTT, suggests that any mixing was minimal after deposition of the YTT. Furthermore, if any of the low D_e values are due to younger intrusive grains, then any bias in age will be minimised by estimating the OSL age from the higher D_e grains contained in the main component, as done here. A constraint on the age of any older intrusive grains can also be obtained, by dividing the main component D_e by the total dose rate determined using the original (bulk) beta dose rate: the resulting age of 78 ± 9 ka for sample J22/4 is not significantly different to that of 71 ± 8 ka listed in Table 1, illustrating the insensitivity of the age estimate to assumptions about mixing. Both of these ages are statistically consistent with that of ~74 ka for the overlying YTT, which supports the sedimentological inference that the palaeosol and associated artefacts date to around the time of the Toba eruption.

Table 1
Dose rate data, D_e values and OSL ages for sediment samples below the Toba tephra, Jwalapuram Locality 22.

Sample code	Dose rates					Equivalent doses					OSL age (ka)
	Beta (Gy/ka)	Beta (Gy/ka) main comp.	Gamma (Gy/ka)	Cosmic (Gy/ka)	Total (Gy/ka)	Grains measured	Grains used	OD (%)	Grains main comp.	D_e (Gy) main comp.	
J22/4	1.57 ± 0.09	1.84 ± 0.10	0.92 ± 0.05	0.14 ± 0.02	2.93 ± 0.15	500	153	35 ± 3	114	209 ± 22	71 ± 8
J22/5	1.22 ± 0.07	1.77 ± 0.08	0.86 ± 0.05	0.12 ± 0.01	2.78 ± 0.14	1000	289	29 ± 2	153	237 ± 12	85 ± 6
J22-2009/2	1.30 ± 0.07	1.42 ± 0.08	0.81 ± 0.05	0.11 ± 0.01	2.37 ± 0.13	900	230	28 ± 3	192	207 ± 11	87 ± 7
J22-2009/1	1.53 ± 0.09	1.77 ± 0.10	0.84 ± 0.05	0.10 ± 0.01	2.74 ± 0.15	800	149	22 ± 3	114	228 ± 20	83 ± 9

The OSL ages of the three deeper samples at Locality 22 are statistically indistinguishable, despite representing ~2.4 m depth of sediment accumulation. The ages are clustered around 85 ka, after which ~1.5 m of sediment was deposited in ~11 ka. This corresponds to an average sedimentation rate of ~13 cm/ka during MIS 5b and 5a. In the absence of any OSL age estimates for the intervening deposits, however, it would not be safe to assume that sedimentation was continuous over this period, especially as the soil isotope data exhibit a shift in carbon and oxygen isotope values within this depth interval (see Section 4 below).

4. Sedimentology and palaeoenvironment

Sedimentological and palaeoenvironmental analyses conducted at Jwalapuram Locality 22 include tephra geochemical characterisation, particle size analysis, magnetic susceptibility, isotopic analysis of soil carbonates, measurement of ^{13}C for the total organic fraction, and x-ray fluorescence (XRF) to determine trace and major element composition. Analyses were conducted at the Research Laboratory for the Archaeology and History of Art, University of Oxford, and the School of Earth and Environmental Sciences, University of Wollongong. For these analyses, a total of 31 samples were collected at 10 cm intervals down the site profile, from depths of 30–330 cm below the surface, shown in Fig. 3. Details of each of the analytical methods are provided in the supplementary online material.

Analysis of the Jwalapuram Locality 22 volcanic tephra layer shows that it is comprised of blocky, non-vesicular glass shards that are mostly 64–78 μm in diameter (Matthews et al., 2012). These glass shards (Table 2) are rhyolitic in composition, with 76.8–78.35 wt% SiO_2, 4.52–5.24 wt% K_2O, 0.65–0.90 wt% CaO, and 0.81–1.20 wt% FeO (anhydrous). The large and explosive Toba caldera in Sumatra, ~2650 km to the southeast, is the closest volcano that could have deposited a rhyolitic ash layer of a few cm depth in India. These precise analyses also fall within the wide compositional range of the Youngest Toba tephra near the source (Chesner, 1998) and at other sites in India (Westgate et al., 1998; Petraglia et al., 2007) (Fig. S1, SOM). The Locality 22 volcanic ash glass shard composition is therefore consistent with the tephra being: (a) sourced from the Toba caldera; and (b) the same as that found at other sites in India. Furthermore, composition of biotite crystals in the distal and proximal deposits confirms the ash was

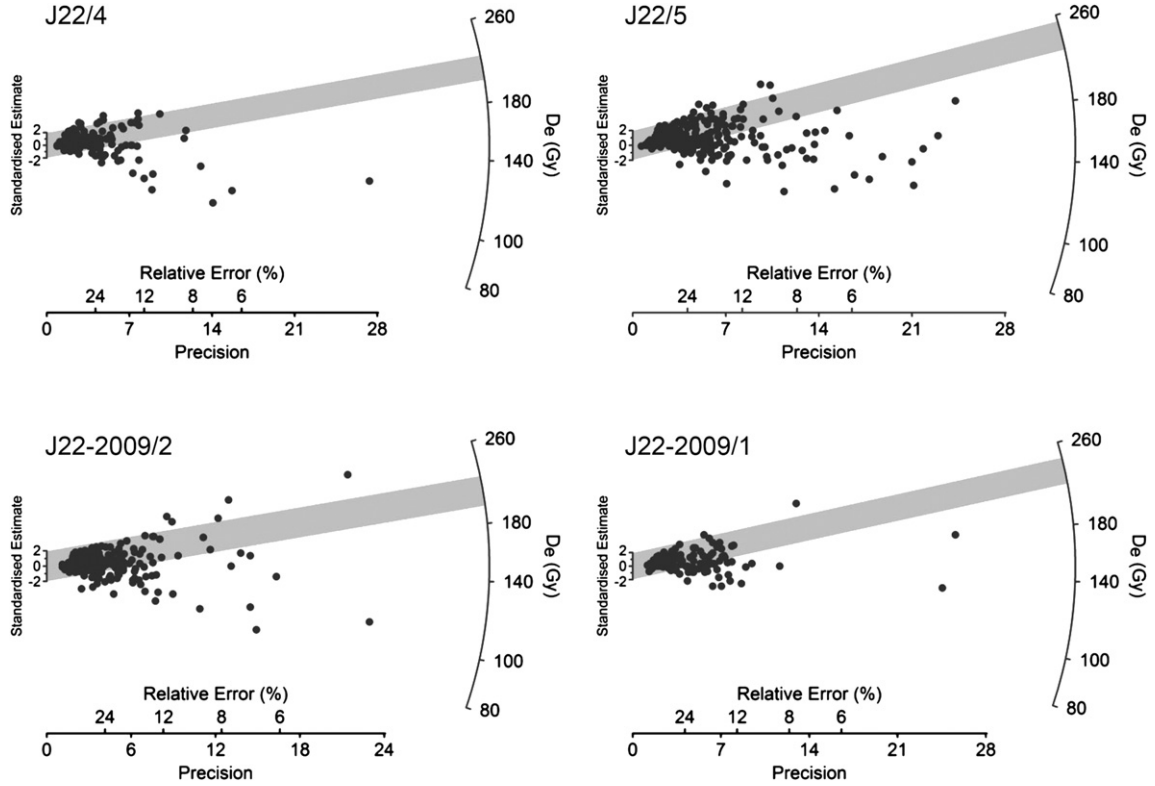

Fig. 4. Radial plots of the D_e values for individual quartz grains of the four OSL samples collected from beneath the YTT at Locality 22. The shaded bands are centred on the D_e values determined by the Finite Mixture Model and used to calculate the OSL ages (see text for details). The majority of grains in each sample lie within the shaded bands.

deposited during the Younger Toba Tuff eruption (Smith et al., 2011) at ~74 ka.

Particle size analysis demonstrates that, broadly, the sediments are poorly sorted and range from very coarse silts to very fine sands, with most samples displaying unimodal particle size distributions. Table S1 (SOM) displays the results of the particle size analysis, and the dry Munsell colour for each sample. The mean particle size for each sample is shown in Fig. S2. The YTT-palaeosol interface occurs between samples SS18 and SS19, at a depth of 200–210 cm below the site surface, which is clearly demonstrated in the particle size results and as a major colour change. The sediments that preserve the YTT layer have the lowest mean particle size of all measured samples, at just under 39 μm. The results also record the larger particle sizes present in the iron and manganese nodule-enriched layers some 60 cm above the palaeosol (c. 130–150 cm depth) as a distinct change, along with even coarser lenses higher in the sequence, particularly at around 70 cm depth. The 130 cm of palaeosol below the YTT layer (the deepest analysed samples) show variation around a mean particle size of 120 μm, indicating fairly consistent parent material and depositional processes for this portion of the sequence. Dry sediments are uniformly reddish yellow above the YTT-palaeosol boundary, but colour changes are more pronounced in the lower samples, shifting between yellowish brown and light yellowish brown at 200–260 cm depth, to brown at 260–300 cm, and then to strong brown at 300–330 cm.

Magnetic susceptibility of all samples is frequency dependent, and the consistently elevated χ_{lf} (low frequency mass-specific susceptibility) readings indicate the presence of a significant component of ultrafine superparamagnetic (SP) ferrimagnetic minerals in the Locality 22 sediments (Dearing et al., 1996). Susceptibility results are presented in Table S2 and Fig. S2. Frequency-dependent susceptibility (χ_{fd}%) values below 10% suggest potential admixture of SP grains and coarser grains, with the SP grains producing the dominant magnetic signal (Dearing, 1999). The YTT-bearing sediments at 190–200 cm depth show similar magnetic readings to those in the upper palaeosol, with a later significant shift between 170 and 190 cm depth.

The lowest mass-specific susceptibility values occur within the upper palaeosol, and increase with increasing depth. χ_{fd}% data for these samples remains within the same range as other samples at the site. Some possible reasons for this lessened signal include decreased iron content from a reduction in biological activity or rainfall, illuviation of iron oxides and oxy-hydroxides down through the soil profile, or excessive waterlogging or porosity (Maher and Thompson, 1995; Marwick, 2005; Blundell et al., 2007). Comparison of the susceptibility results to the iron content as measured by x-ray fluorescence (Fig. S2; Table S3) suggests that illuviation is the cause, which marks the palaeosol as a relatively mature soil profile developed over a significant period of time. This finding supports the notion that the palaeosol was well-established at the time of the YTT eruption, and the similarities in susceptibility across the YTT-palaeosol boundary suggests that some topsoil sediments were entrained during the period of YTT redeposition seen at Locality 22.

Isotopic analysis of soil carbonates and soil organic fraction below the YTT layer shows variation over the 120 cm sampled section (Table 3 and Fig. 5). Broadly, the sequence can be split into two periods, with a shift between 280 and 290 cm depth. For the soil carbonates this shift is concordant in both the carbon and oxygen records, indicating change from a landscape with higher proportion of C_4 grasses and a cooler/drier and more evaporative climate to an environment with an increased C_3 woodland/grassland component and decreased evaporation. However, whereas the upper portion of the ^{13}C record from the organic fraction tracks that from soil carbonates (with an offset of 12–13%) and supports assessment of mixed C_3/C_4 vegetation, the lower portion deviates from the carbonate record, suggesting more complicated processes affecting the site below 280 cm depth. The discrepancy may in part occur for chronological reasons, with the ^{13}C organic fraction contemporaneous or older than the enclosing sediment, and the carbonate modules post-dating sediment deposition. In any case, this has not affected the results from the artefact-bearing upper palaeosol, which is relatively stable in its isotopic composition. The

Table 2
Average major element composition (% with standard deviation in brackets) of tephra glass shards, 200 cm depth, Jwalapuram Locality 22.

	JWP22–SS18 (200 cm depth)	
	Average	±1σ
SiO_2	77.22	(0.38)
TiO_2	0.06	(0.04)
Al_2O_3	12.46	(0.12)
FeO	0.99	(0.11)
MnO	0.07	(0.04)
MgO	0.06	(0.02)
CaO	0.77	(0.09)
Na_2O	3.23	(0.35)
K_2O	4.99	(0.22)
P_2O_5	0.01	(0.01)
Cl	0.15	(0.01)
n	15	

Table 3
Soil carbonate stable isotope and $\delta^{13}C$ organic fraction results from below the Toba tephra, Jwalapuram Locality 22.

		Soil carbonates		Soil organic fraction
Sample	Depth (cm)	$\delta^{13}C‰_{vpdb}$	$\delta^{18}O‰_{vpdb}$	$\delta^{13}C$
SS19A	210	−5.938	−2.934	−18.81
SS19B	210	−6.159	−2.181	
SS19C	210	−6.974	−2.681	
SS20A	220	−6.866	−4.093	−19.15
SS20B	220	−5.635	−3.303	
SS20C	220	−6.615	−3.839	
SS21A	230	−6.319	−2.298	−18.94
SS21B	230	−6.279	−2.160	
SS21C	230	−6.521	−2.404	
SS22A	240	−6.228	−3.392	−18.71
SS22B	240	−6.075	−2.980	
SS22C	240	−6.019	−3.212	
SS23A	250	−6.017	−2.117	−18.55
SS23B	250	−6.075	−2.133	
SS23C	250	−5.964	−2.285	
SS24A	260	−4.424	−1.027	−19.10
SS24B	260	−6.943	−1.879	
SS24C	260	−5.938	−1.678	
SS25A	270	−6.319	−2.170	−19.80
SS25B	270	−6.699	−2.390	
SS25C	270	−6.044	−2.108	
SS26A	280	−6.730	−2.323	−18.82
SS26B	280	−6.586	−2.409	
SS26C	280	−6.594	−2.372	
SS27A	290	−4.628	−1.176	−20.11
SS27B	290	−4.534	−1.094	
SS27C	290	−4.039	−0.871	
SS28A	300	−4.526	−1.010	−19.67
SS28B	300	−4.476	−1.005	
SS28C	300	−4.390	−0.974	
SS29A	310	−3.942	−0.847	−22.01
SS29B	310	−3.826	−0.789	
SS29C	310	−3.900	−0.926	
SS30A	320	−4.604	−1.111	−21.77
SS30B	320	−4.576	−1.094	
SS30C	320	−5.465	−1.518	
SS31A	330	−5.562	−1.465	−21.00
SS31B	330	−5.330	−1.342	
SS31C	330	−5.585	−1.528	

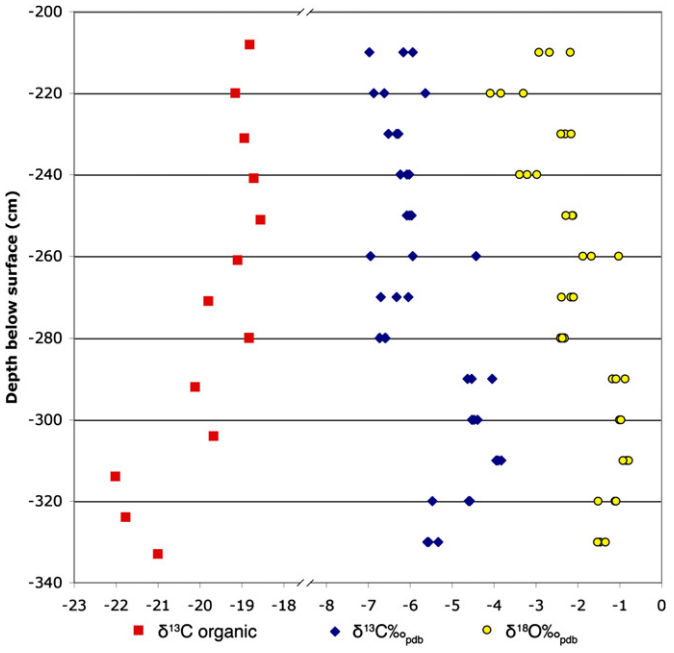

Fig. 5. Soil stable isotope results from the total organic fraction ($\delta^{13}C$ organic) and soil carbonates ($\delta^{13}C_{‰pdb}$ and $\delta^{18}O_{‰pdb}$) below the Toba tephra, Jwalapuram Locality 22.

change at 280–290 cm depth does not correspond to a stratigraphic or sedimentary break at the site, as shown by continuity in the sedimentological and magnetic susceptibility data, pointing to a climatic influence. One possibility is the change from stadial MIS 5b to the warmer MIS 5a, which occurred around 85 ka in southern India (Pattan and Pearce, 2009).

There are also minor trends within each of the isotopically-identified periods, with the earlier portion of the record and the very top of the sequence trending slightly towards drier conditions. The latter coincides with the period leading up to the Toba eruption, which occurred during the climatic downturn following MIS 5, and specifically during the cooler period between Dansgaard-Oeschger interstadials 20 and 19 (Haslam and Petraglia, 2010). These minor trends are indicative only and not conclusive, however, and require further testing to examine their implications. In general, the three carbonate nodules from each depth show tight clustering, suggesting that variability across the sampled area was reasonably limited at any particular point in time. However, as the sampled area may be spatially restricted to perhaps only tens or hundreds of square metres, the results from Locality 22 cannot be extrapolated to other regions: again, more comprehensive sampling within the Jurreru Valley is required to examine the representativeness of these results.

Keeping in mind the above caveats, the ^{13}C isotope data allow initial interpretations regarding the vegetation at Locality 22 during the sampled interval (for detailed explanations of the relationship between soil carbon isotopes and vegetation see Cerling, 1984; Mariotti and Peterschmitt, 1994; Andrews et al., 1998; Sikes et al., 1999; Williams et al., 2009). Data from the earlier period (corresponding to 290–330 cm depth) suggest that C_4 grasses made up ~45–60% of the floral biomass at that time, with the potential presence of C_3 grasses (Sukumar et al., 1995; Rajagopalan et al., 1997) meaning these figures should be considered minima only. For the later period leading to the Toba eruption (equivalent to 210–280 cm depth), the data indicate that C_4 grasses decreased to a minimum of ~30–45% of the biomass. Both of these C_3/C_4 ratios may be considered as representing grassy woodlands (Sikes et al., 1999), although in the earlier period the vegetation would have been more open and, in the later period, increased woodlands within this portion of the Jurreru Valley may have offered greater shade cover to hominin groups. Soil carbonate nodules are more abundant in the sediments below the YTT layer than within and above this layer, which may be an indication of decreased moisture following the eruption.

Results of the sediment geochemistry study (Table S3) show that shifts in sediment trace and major element composition are coincident for the most part with stratigraphic breaks identified in the field and via granulometry. The focus here is on a subset of elements that have been shown in previous studies to be potentially influenced by human occupation (Cu, Sr, Ba, Ca), as well as other elements that track stratigraphic changes, and especially the distinct YTT layer, at Locality 22 (Rb, As, V, Pb, Th). Full discussion of the complex records recovered for both major and trace elements in the Locality 22 sequence will be presented elsewhere. The XRF results are shown in Fig. S3, and demonstrate depletion of Cu, Sr and V in the YTT deposit, while values for Pb, Th, Rb and As are sharply elevated in the same interval, just above 2 m in depth. Most of the presented elements also display dips in concentration towards the top of the sequence, where the influence of modern soil formation processes is likely more prevalent. A change in sediment input or leaching conditions is seen at around 100–120 cm in several of the datasets, matching a similar excursion in the magnetic record. Perhaps the most interesting results from the perspective of occupation at Locality 22 are the strong Ba and Ca signals that mark the palaeosol at 200–250 cm depth. Both barium and calcium have been suggested as a potential indicators of human waste disposal in more recent contexts (Wilson et al., 2008). While their utility in Late Pleistocene Indian contexts has yet to be established, the Locality 22 results suggest that further exploration of the links between these elements and stable palaeosols supporting Pleistocene hunter-gatherer habitation is warranted.

Initial phytolith results are here considered for one sample, collected from the Jwalapuram Locality 22 palaesol at 202–212 cm depth. Phytoliths observed in this level help to reconstruct the basic site flora at the time of the Toba eruption and during site occupation (Fig. S4). This sample includes a high concentration of Festucoid types (41.3%), with more square, rectangular, spherical (Amaranthaceae/Chrysobalanaceae), nodular (Arecaceae/Bombacaceae) and oblong phytoliths than Panicoid dumbbells (Gramineae/Panicum; 8%) and Chloridoid saddles (Gramineae). The frequency of trichomes (24%) is noteworthy, and includes mostly long pointed hair cells (Burseraceae/Fabacea). Bulliform phytoliths of square (Gramineae) and rectangular (Euphorbiaceae) types are present (5.3%); there was no observation of fan-shaped morphotypes. The presence of silicified woody elements (7.3%) indicates the presence of trees and shrubs. Together these data suggest a grassy woodland environment at the time of the Toba eruption, supporting the reconstruction based on soil carbonate isotopes.

5. Palaeotopography and artefact distribution

The combination of mature soil development, dense artefact accumulation and evidence of termite activity at the tephra–palaeosol interface indicate that the cultural horizon was exposed to the air and undergoing active pedogenesis at the time of the ash fall. Reconstruction from artefact positions on the palaeosurface (Fig. 6a) shows a relatively horizontal area with slight topographic variations and a gentle slope downwards to the east. Note that the eastern portion of this reconstruction is at lower resolution, as it uses depth data averaged to the nearest ~2 cm (recorded manually), while for the remainder of the site depths are to the nearest millimetre (recorded via total station).

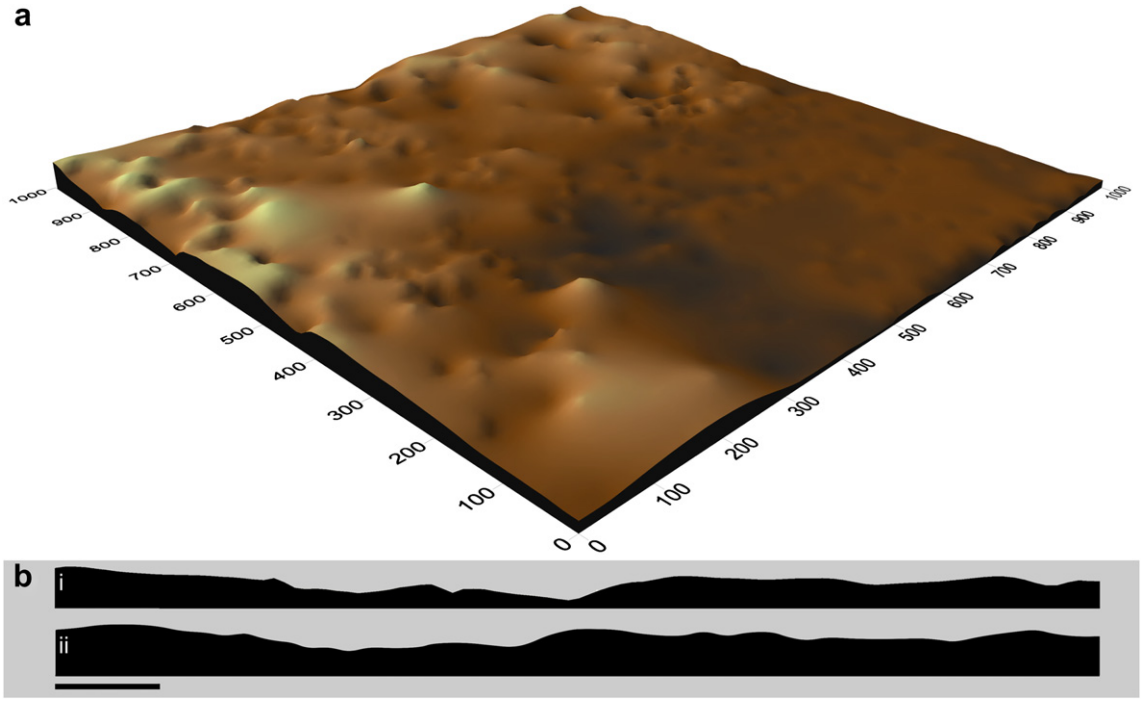

Fig. 6. (a) Reconstructed palaeosurface underlying the YTT deposits, facing north, Jwalapuram Locality 22, measurements in cm; (b) comparison of northwest YTT-palaeosol stratigraphic boundary contour based on reconstruction from (i) artefact depths and (ii) site stratigraphic profile, scale is 1 m.

As a measure of the accuracy of these data, the profile at the edges of this reconstruction can be compared to the contour of the YTT-palaeosol interface stratigraphic boundary recorded at the site following excavation. These demonstrate a close fit (Fig. 6b), and provide a further degree of confidence in the conclusion that the uppermost artefacts in the palaeosol mark an occupied surface that was exposed at the time of the eruption. The palaeosurface did not show any morphological or sedimentological evidence of scour channels or erosional cuts either during excavation or in the reconstructed topography. The Jurreru Valley silts are prone to minor displacement by mammalian herds when saturated during the annual monsoon rains (Eren et al., 2010), and the negligible mixing of Toba tephra into the upper palaeosol, combined with the absence of evidence for artefacts moving upwards into the tephra layer, may indicate that neither large herbivores nor termites were active at the site immediately following the Toba eruption.

Artefact distribution likewise shows no patterning that may be indicative of disruption prior to the ash fall. Plotting artefact positions by weight demonstrates that they are not size-sorted either vertically (Fig. 7) or horizontally (Fig. 8a), indicating that post-depositional movement is not a significant factor at the site. The distribution of artefact classes within the palaeosol (Fig. 8b) demonstrates that the highest concentrations are found in the eastern half of the site, although both retouched and unretouched limestone flakes are distributed across the excavated area. There is no apparent pattern to the distribution of non-limestone (chert and dolerite) flakes. Hammerstones form a rough outline surrounding the most densely-clustered portion of the site, with cores located both close to and away from these. Portions of the site with little to no artefact discard (including the southern corner and other patches to the north and west) are intriguing, with one possibility being that they record sites of vegetation presence at the time of the Toba eruption. The presence of cores, hammerstones and lithic debitage across the Locality 22 palaeosol attests to its extended use as a reduction locale, with material transported from the southern valley flank before being knapped, used and fashioned further out in the valley bottomlands. This pattern and the density of remains suggest that Middle Palaeolithic hominin groups were repeatedly returning to the same location, bringing with them raw materials and tools for flake production.

6. Lithic technology

The Locality 22 assemblage consists of 1628 artefacts classified into a wide range of core, flake and retouched flake types as shown in Table 4 and Fig. 9. The assemblage is Middle Palaeolithic in character with evidence of prepared cores, expedient cores and retouched flakes of highly variable retouch type and location, including scrapers and points.

6.1. Raw Materials

The assemblage is made up almost entirely of cherty limestone (94%) collected from the southern flank of the Jurreru Valley, approximately 900 m from the excavation. The stone is available as tabular or sub-rounded pieces on the hillsides and valley floor, and varies greatly in quality. The best pieces possess excellent fracture qualities, however some display minor laminations, and this has likely affected the way some pieces were worked.

Dolerite is the next most abundant stone (3.8%) and outcrops as a dyke along the upper margin of the same southern flank, with the nearest access also less than 1 km from Locality 22. Dolorite nodules appear to have been brought to the site to serve as hammerstones, and both intact hammerstones and fragments are present. Very small quantities of quartzite, quartz, crystal quartz ochre, and chalcedony artefacts also occur in the assemblage (Table 5). Raw material procurement at Locality 22 is therefore predominantly local, and the same pattern was noted at the nearby Locality 3 site to the east (Haslam et al., 2010b) where artefacts beneath the Toba tephra are dated to between 77 and 74 ka.

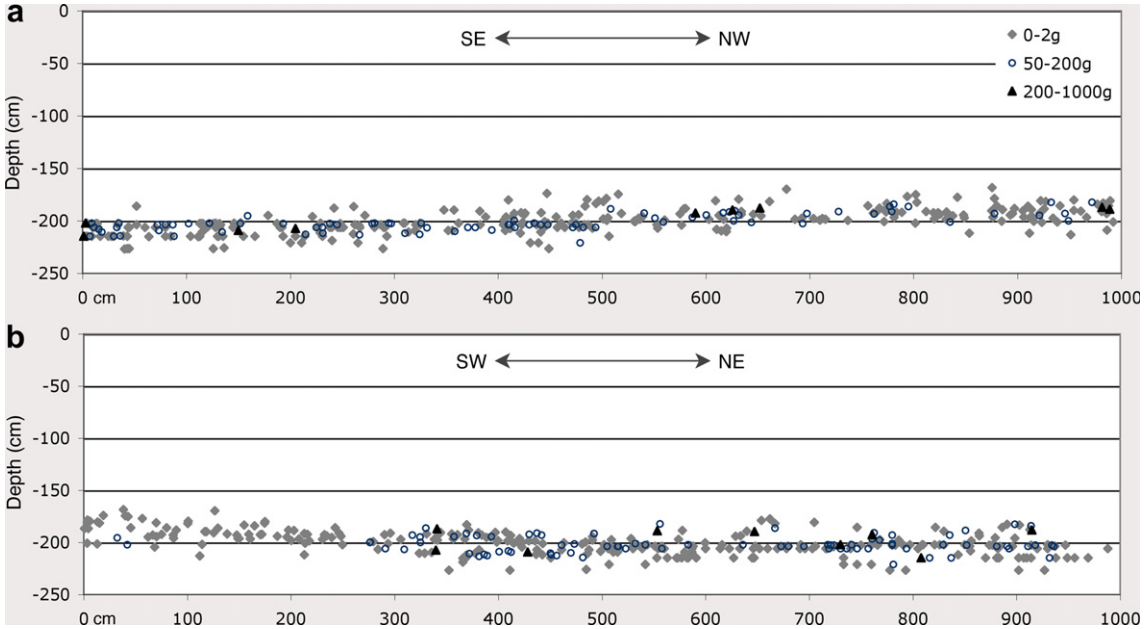

Fig. 7. Vertical artefact distribution by weight class, below Toba tephra, Jwalapuram Locality 22. The charts show the distribution along two axes: (a) SE-NW, and (b) SW-NE, indicating the general palaeosol slope from west to east. As the charts each compress 10 m of slightly sloping horizontal distribution, the vertical concentration is actually even tighter than illustrated.

6.2. Core technology

The assemblage contains 50 cores classified into 12 technological types (Table 4), all of which are made from the local limestone. Levallois and multiplatform cores dominate the core assemblage, but discoidal and semi-discoidal (i.e. defined as bifacial radial cores with discontinuous flaking around the perimeter), single platform and bidirectional cores are also present, along with core fragments and nodules with very few flake scars.

Cores show widely varying levels of reduction. Core mass, proportions of cortex remaining and numbers of flake scars on cores indicate that single platform cores are often the least reduced and that discoidal, bidirectional and multiplatform cores generally show far greater levels of reduction, with Levallois cores showing

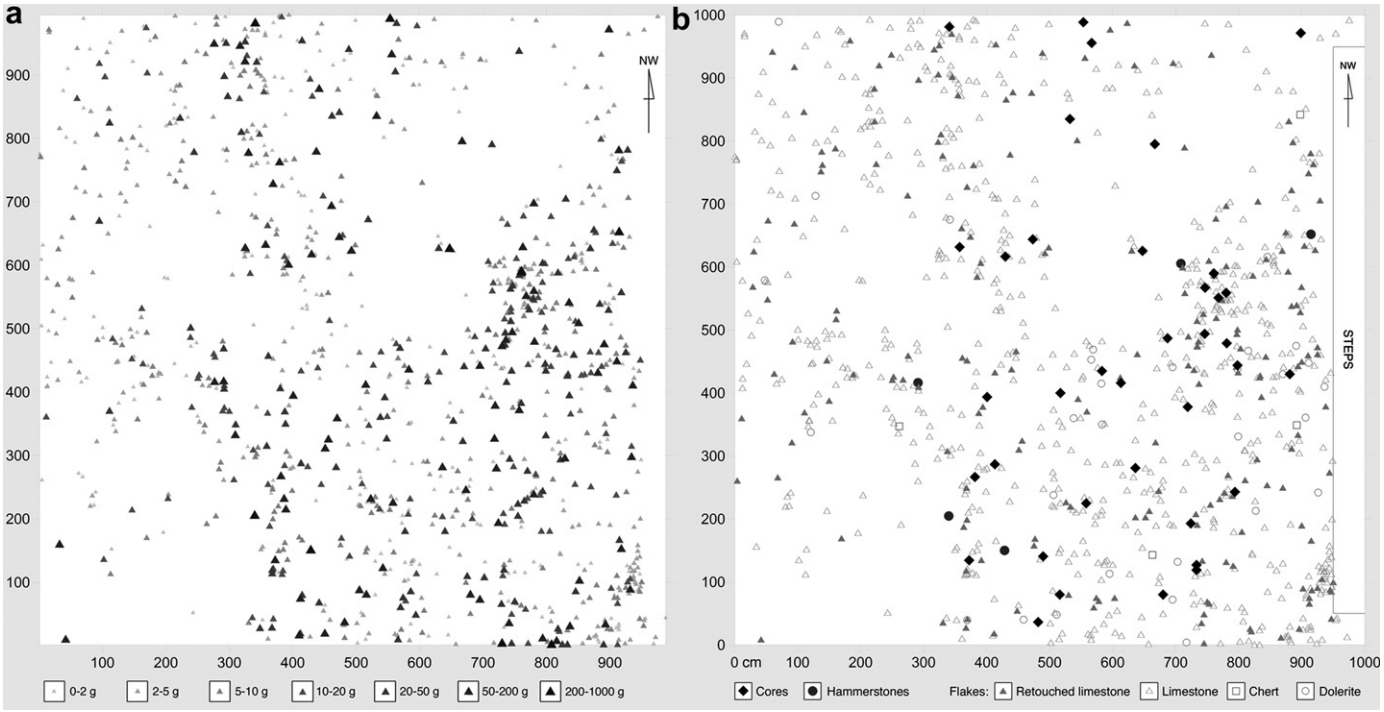

Fig. 8. (a) Plan artefact distribution by weight class, below Toba tephra, Jwalapuram Locality 22. Heavier artefacts have larger and darker symbols, with axes in cm. (b) Plan distribution of cores, flakes and hammerstones below the Toba tephra, Jwalapuram Locality 22, with axes in cm and the unexcavated steps area to the northeast marked.

Table 4
Number and percentage of each lithic artefact type, Jwalapuram Locality 22.

Type	Total	%
Cores		
Levallois Core	10	0.61
Multiplatform Core	8	0.49
Core Fragment	6	0.37
Single Platform Core	6	0.37
Bidirectional Core	4	0.25
Semi-Discoidal Core	6	0.37
Discoidal Core	3	0.18
Biface	1	0.06
Discoidal Core Fragment	2	0.12
Faceted Unidirectional Core	1	0.06
Microblade Core (Above Ash)	1	0.06
Flaked Slab	1	0.06
Flake Types		
Flake	1157	71.07
Flaked Piece	142	8.72
Blade	14	0.86
Redirecting Flake	7	0.43
Eclat Debordant	5	0.31
Hammerstone	5	0.31
Levallois Flake	2	0.12
Microblade	1	0.06
Ridge Straightening Blade	1	0.06
Retouched Flakes		
Broken Retouched Flake	62	3.81
Side Retouched Flake	43	2.64
End Retouched Flake	24	1.47
Notched Retouched Flake	22	1.35
Side and End Retouched Flake	18	1.11
Double Side and End Retouched Flake	12	0.74
Double Side Retouched Flake	9	0.55
Notched Double Side and End Retouched Flake	6	0.37
Retouched Flaked Piece	6	0.37
Double Side and Double End Retouched Flake	5	0.31
Double Side and End Retouched Flake	4	0.25
End Retouched Flake on Break	4	0.25
Burin	3	0.18
Notched Side Retouched Flake	3	0.18
End Scraper on Redirecting Flake	2	0.12
Notched End Retouched Flake	2	0.12
Notched Side and End Retouched Flake	2	0.12
Notched/Denticulated Retouched Flake	2	0.12
Side and Double End Retouched Flake	2	0.12
Side Retouch on Blade	2	0.12
Double End Retouched Flake	1	0.06
Double Side Scraper on Blade	1	0.06
Double Side Scraper on Redirecting Flake	1	0.06
Notched Levallois Flake	1	0.06
Side and End Retouch on Blade	1	0.06
Side and End Retouch on Break	1	0.06
Side Retouch on Blade Fragment	1	0.06
Side Retouch on Levallois Point	1	0.06
Tanged Retouched Flake	1	0.06
Points		
Bifacial Point	1	0.06
Tanged Point	1	0.06
Unifacial Point	1	0.06
Total	1628	

medium levels of reduction (Figs S5–S7, SOM). Both single platform and Levallois cores produced the largest flakes immediately prior to discard, consistent with lower levels of reduction, however the largest scar length found on cores is positively correlated with core size ($r^2 = 0.795$).

Single platform cores were typically formed by striking a naturally flat surface on a semi-angular nodule, working the face unidirectionally until increasing platform angles or the build up of step terminations resulted in discard. Judging from the lower scar counts, larger core sizes and greater proportions of remaining cortex, many single platform cores appear to have been discarded quite early in the reduction process; however, some cores were later rotated, either by adding a platform on the distal end to create bidirectional cores, or rotating the core several times to make use of viable platforms. This process of rotation sometimes removed old platform edges which are preserved on the dorsal surface, here termed redirecting (also known as core trimming) flakes. Rotating single platform cores was probably a means of extending the reduction potential of the core when problems appeared with the original platform and core face.

Levallois cores show single preferential removals as well as recurrent unidirectional flaking and more rarely recurrent centripetal flaking. Fig. 10 shows annotated 3D scans of four Levallois cores showing the order of large flake removals and the presence of faceting on the main prepared platforms. Such cores appear to have had distal and lateral convexities formed via radial flaking of the upper (debitage) surface before by one or more large flakes were struck from a faceted platform. Levallois removals often show hinge terminations or even overshot flaking. The use of thin tabular or sub-rounded pieces means that some cores become very thin once several large flakes are removed, often with only minimal flaking on the lower (platform) surface to create a steep faceted platform for removals from the upper surface. Fig. 10, B–D provides examples of large recurrent Levallois flake removals from thin tabular or sub-rounded nodules. Sometimes these removals encroached upon the edge of the core, likely resulting in removing éclat debordant flakes, as in Fig. 10, C–D.

Discoidal and radial cores show a pattern of alternating radial flaking on the upper and lower surfaces, which is sometimes steep on both sides or steep on one and shallow on the other (e.g., Fig. 11). Faceting is almost entirely absent and blows were typically directed onto flat areas or intersecting flake scar ridges to create flakes with plain or dihedral platforms that terminate at or just short of the centre of the upper or lower core face.

Initial microscopic functional analysis of the Locality 22 assemblage demonstrates that cores were on occasion re-used as tools. One discoidal limestone core, recovered at a depth of 207 cm from the eastern portion of the site and dated with the rest of the assemblage to ~74 ka, retains residue resulting from a scraping activity (Fig. 12). The residue forms a granular, dark red to orange film in three locations near one of the artefact edges, and adheres to relative topographical highs on the artefact surface, supporting a functional assessment of scraping a hard contact material. Lineations within the residue indicate the direction of artefact motion during use.

6.3. Flake characteristics

The flake assemblage shows a high degree of fragmentation, with only 16% of flakes being complete. Edge damage from trampling or some other post-depositional process is common but artefacts show no signs of rolling or water transport. Data on certain dimensions has been included from broken specimens where appropriate. For example, proximal and platform dimensions are given for complete and proximal fragments with intact platforms, and distal measurements are for complete and distal fragments. Complete flakes at Locality 22 have a mean length of 23 ± 16 mm, but numerous flakes are larger than 50 mm with the longest flake measuring 112 mm. On average flakes are not particularly elongate (length:width = 1.2 ± 0.8), are thin relative to length (length:thickness = 3.3 ± 1.4) and flat relative to width (width:thickness = 3.1 ± 1.5), typically possess at least one dorsal ridge running parallel to the percussion axis, and retain some cortex (mean 18 ± 32%).

Platforms are typically large, at around one-third the size of the ventral surface, consistent with hard hammer blows being set in

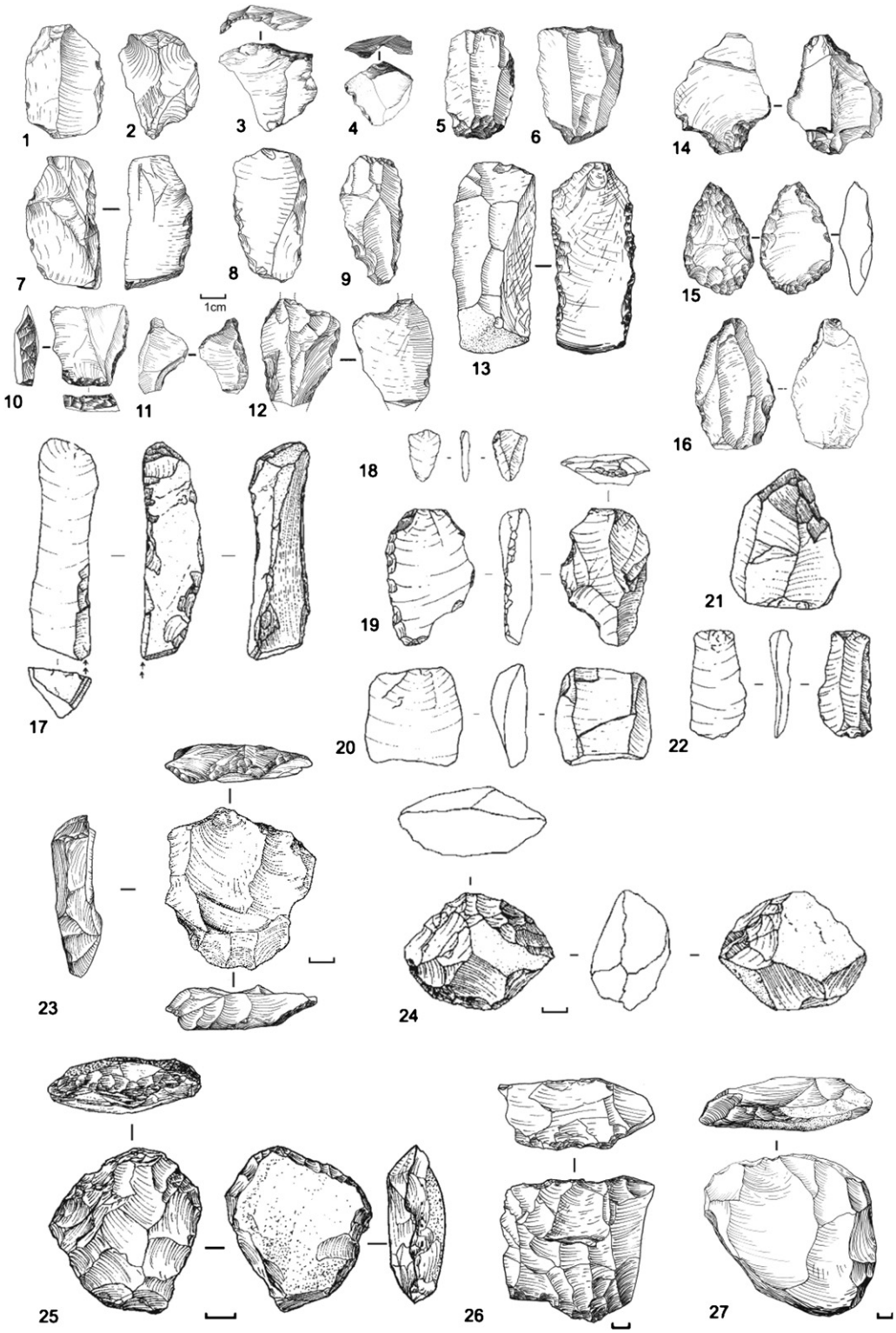

Fig. 9. Examples of flakes, retouched artefacts and cores, Jwalapuram Locality 22. 1. Side and end retouched, 2. Levallois flake, 3. Flake from faceted core, 4. Flake from discoidal or Levallois core, 5. End retouched, 6. Double end retouched, 7. Side retouched, 8. Side retouched, 9. Double side retouched, 10. Éclat debordant, 11. Tanged flake, 12. Broken possible tanged scraper or point, 13. Double side retouched, 14. Broken tanged point with possible impact fracture on tip, 15. Bifacial point, 16. Bifacially retouched point with impact fracture on tip, 17. Burin on blade, 18. Levallois point, 19. Side retouched Levallois flake, 20. Flake from bidirectional core, 21. Blade, 22. 23. Recurrent unidirectional Levallois core on flat slab, 24. Semi-discoidal core, 25. Recurrent centripetal Levallois, 26. Bidirectional core on flat slab, 27. Recurrent unidirectional Levallois core.

from the platform edge. Platform surfaces are often formed from single (49%) or multiple flake scars (30%). Dihedral and cortical platforms are each found on 7% of flakes, while crushed platforms are rare at 4%. Tiny focalized platforms that result from blows positioned on the extreme edge of the core account for only 2% of flakes. Roughly half (51%) of the intact platforms present in the assemblage show no signs of platform preparation. Overhang removal is found on 35% of specimens and faceting is present on

Table 5
Breakdown of lithic artefacts by raw material type, Jwalapuram Locality 22.

Raw Material	Total	%
Limestone	1528	94.0
Dolerite	61	3.8
Chert	17	1.0
Quartzite	13	0.8
Chalcedony	4	0.2
Quartz	2	0.1
Ochre	1	0.1
Total[a]	1626	

[a] Raw material was not recorded for two artefacts.

17% of platforms. These statistics are consistent with the removal of flakes from a variety of core types described above.

Dorsal surfaces show a variety of scar directions, consistent with the diversity of core reduction strategies. Scars originating from the proximal end are the most common (73%), followed by radial scar patterns (16%). Flakes with radial scar patterns are significantly larger on average than those with proximal orientations (mean proximal = 20 mm, mean radial = 27 mm, df = 123, $p = 0.015$), consistent with the production of much larger than average flakes from Levallois cores. Another 16% of flakes have both faceted platforms and proximal and non-proximal/non-radial orientations, suggesting that some of these flakes may derive from recurrent unidirectional Levallois cores where a range of flake scar orientations is possible. Bidirectional scar patterns are only found on 6% of flakes, whereas single direction orientations that do not originate from the proximal end (e.g., from left, right and distal) make up around 3.6% of cases. Flaking originating from a central ridge, as in redirecting flakes or flakes that remove the edge of a radial core (éclat debordant), are present in 0.4% of cases. Less than 1% of flakes are purely cortical, indicating a low incidence of primary core reduction at Locality 22 and suggesting that removal of cortical surfaces was taking place at the raw material source, with cores transported to the site in a partially-reduced state. This is somewhat unexpected given the proximity to source.

6.4. Retouched flakes

Forms typically identified as scrapers and notches dominate the retouched assemblage, though any specific functional interpretation is eschewed until use-wear and residue analyses are completed. Summary statistics for the retouched artefacts are presented in Table S5. Retouched flakes are typically nearly double the length of unretouched flakes (39.9 ± 16.8 mm vs. 22.8 ± 13.1), suggesting larger flakes were specifically chosen for use. Retouching is characterised by steep (73 ± 11°) and sometimes abrupt sections of the lateral and distal margins, with and without notches. In some cases, isolated, pronounced and complex notches occur on an edge. The retouch is usually systematic and isolated to a single portion of the margin or face, but there is evidence of damage to edges in numerous cases that may not be caused by deliberate retouch. Trampling by humans or large animals is a possibility (Eren et al., 2010). Well-defined end scrapers are common, and several seem to be made on the distal or both distal and proximal ends of snapped flakes. Retouch intensity, measured by the geometric index of unifacial reduction (Kuhn, 1990) indicates edges are moderately retouched (0.53 ± 0.27), whereas around 50% of the perimeter is retouched in most cases.

6.5. Points

At least three likely points are present below the ash at Jwalapuram Locality 22 (Fig. 9), while two flakes with broken stems may

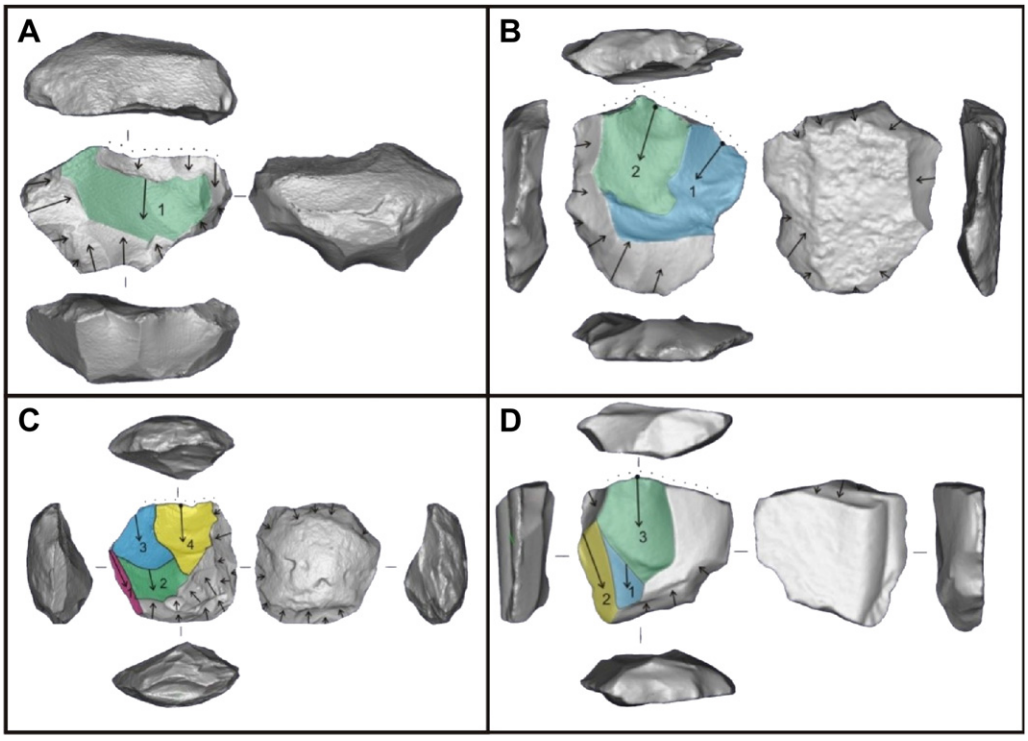

Fig. 10. A) Single preferential Levallois flake removal with subsequent flaking of the upper core surface, perhaps representing an abandoned attempt to re-prepare the core for a second Levallois removal. B) Recurrent unidirectional Levallois core showing two large overlapping flake removals both ending in hinge terminations. The core is made on a flat tabular piece of limestone with minimal flaking on the underside. C) Recurrent unidirectional Levallois core with the final flake ending in a hinge termination. D) Recurrent unidirectional Levallois core most likely made on the ventral surface of a large flake. Dotted lines show the location of platform faceting.

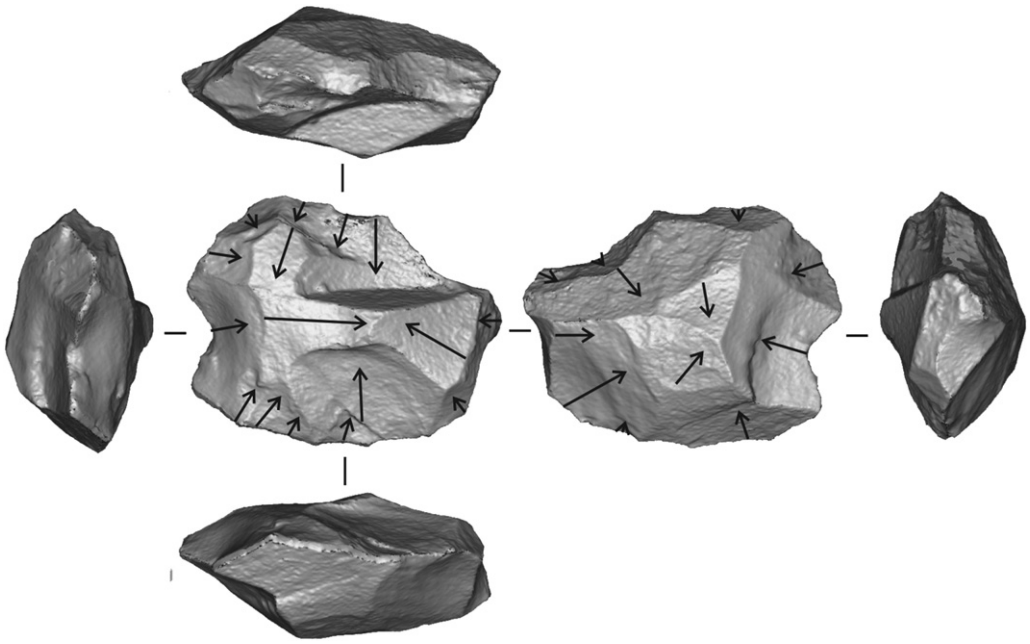

Fig. 11. Discoidal core that may once have been a recurrent Levallois core, Jwalapuram Locality 22 palaeosol.

also be tanged points or scrapers. One is clearly deliberately tanged, with extensive, steep ventral retouch on either side of the bulb of percussion, forming a tang of around 1 cm in length. The original faceted platform surface can be seen on the proximal end. The distal end is snapped, possibly as a result of impact. The point is broken into two conjoining pieces, but the fresher surface of the break suggests this took place post-depositionally. The bifacial point is thick, but extensively invasively flaked on the dorsal surface, with marginal flaking around the perimeter of the ventral surface. A third point is marginally retouched along the left dorsal margin, as well as along the right ventral margin. A distinctive impact fracture appears on the ventral tip. The Locality 22 points all have high tip cross-sectional area (TCSA) scores (ranging from 100 to 232) that would put them in the hand thrown or thrusting spear range (Shea and Sisk, 2010; Costa, 2011). However, the use of TCSA to determine point function is purely hypothetical and does not preclude use of these points in other ways.

7. Middle Palaeolithic occupation at Jwalapuram Locality 22

The combined archaeological and palaeoenvironment results indicate that hominins using the Locality 22 site prior to the eruption of the Toba caldera inhabited a mixed woodland/grass environment, with the local climate trending towards cooler and likely drier conditions immediately prior to the eruption. These findings support similar data from below the Toba tephra at

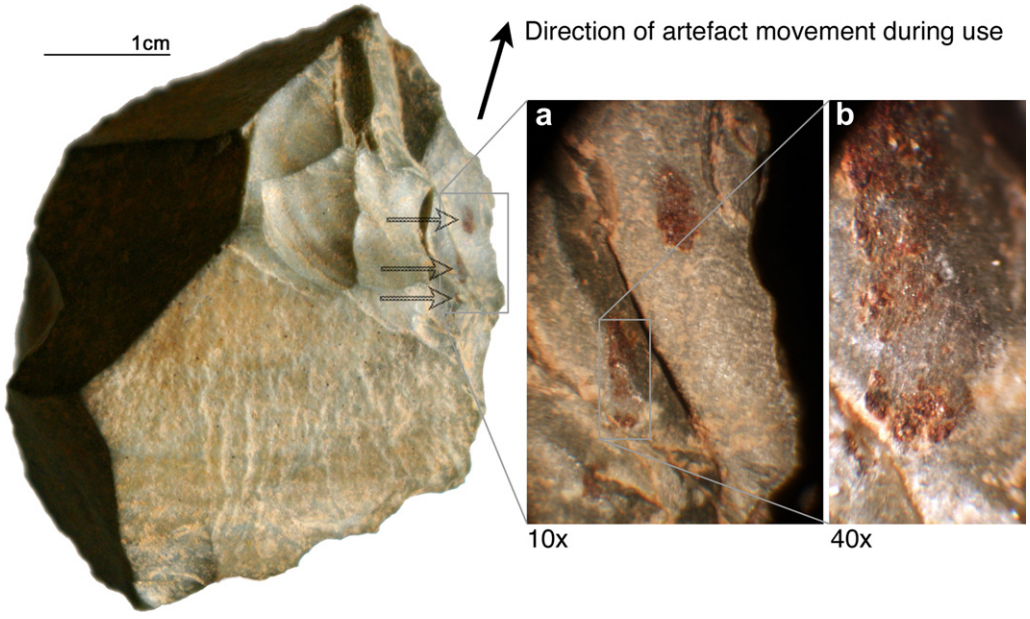

Fig. 12. Residues (arrowed) and use-wear on a limestone discoidal core from below the Toba tephra, Jwalapuram Locality 22.

Jwalapuram Locality 3 (Haslam et al., 2010b), and demonstrate sustained habitation of the Jurreru Valley leading up to the Toba event.

Locally-based hominin groups selected limestone and other raw materials (e.g., dolerite, quartzite) from the valley slopes, reducing some close to the valley margins (Petraglia et al., 2009b) and bringing, in other cases, both nodules and hammerstones out onto the valley floor for further reduction. Various stages of the reduction continuum are present, including early and late stage single platform and generally later stage multiplatform cores, and flakes are also retouched to differing degrees, indicating that reduction was likely of differing frequency and duration. Given the ready availability of raw materials in the valley, differential reduction is unlikely to be the result of raw material scarcity or transport costs and suggests instead that significant time was spent in technological activities such as core reduction and implement manufacture and use at the site. Initial functional analysis of a small sample of artefacts has detected traces of maintenance activities and further analyses will expand the understanding of the range of tasks performed at the site. Flakes were largely not standardized in size, shape and production technique, and were retouched in to a range of ways that probably point to diverse function.

Mapping of major sedimentary units and the position of present-day Toba tephra emplacements indicate that the Locality 22 site was situated south of, but relatively close to, the Jurreru River at the time of its occupation, with a depressed lacustrine or marshland environment periodically present a few hundred metres at most to the east. Initial palaeotopographical survey using the tephra as a marker (Blinkhorn et al., 2012) indicates that the Locality 22 palaeosurface was slightly elevated relative to areas to the north and east, possibly owing to colluvial input from the medial ridge situated to the west of the site (Fig. 1). It is probable, therefore, that the occupants of Locality 22 were well placed to observe both game and predator activity across much of the valley bottomlands, while remaining close to water sources while they worked. This choice placement in the landscape might also explain the presence of likely spear points at the locality. Published (Haslam et al., 2010c) and unpublished Late Pleistocene data from excavations in the Billa Surgam caves, 13.5 km north-northeast of Locality 22, indicates that larger vertebrates in the Jurreru in the lead-up to the Toba eruption may have included the ungulates *Boselaphus*, *Equus*, *Tetracerus*, *Rhinoceros* and *Axis*.

Surveys and excavations in the Jurreru Valley have yet to reveal unambiguous evidence for Middle Palaeolithic sleeping or cooking sites, and it is not apparent, therefore, whether Locality 22 represents a typical habitation site or a more restricted-use lithic reduction and processing area. Eight fire-cracked rocks were recovered at the site (three of dolerite, five of limestone), but it is not known if these were brought to the site in this condition or resulted from natural or cultural fires on site. The low magnetic susceptibility results for the upper palaeosol point to transport to the site as a more likely explanation.

From the quantity of lithic debitage and evidence for repeated site use for lithic reduction, it is reasonable to propose that Locality 22 would most likely have been a clear, flat, grassed area, perhaps overshadowed by isolated trees, with views across the surrounding grasslands to the river and valley slopes, and more limited visibility eastwards out of the valley to the open plains beyond. The site, in turn, would have been clearly visible from much of the valley flanks, presenting a central gathering point to which hominins could bring raw materials and possibly food. The position of the Jurreru Valley as a large, well-watered pass through the locally elevated quartzite and limestone beds would have channelled faunal movements in an east-west direction. Combined with reliable stone sources, this suggests that the valley's occupants would not have needed to range more than a few kilometres to access critical resources. This conclusion is commensurate with the hypothesis that Locality 22 supported repeated and focused visits rather than random discard of materials or short-term site-use. Despite systematic survey (Shipton et al., 2010), there is currently a lack of evidence for Middle Palaeolithic activity on either the valley slopes or the quartzite plateaus. While this does not preclude their use as viewpoints or for short-term activities, it suggests that the higher ground was not being regularly used for knapping activity. The potential remains, therefore, for further centralised locales to be found at strategic points on the valley floor. At the time of the Toba eruption, such sites may have occupied a similar topographic position elsewhere on the margins of the (at least seasonally) watered depression to the east of Locality 22 (Blinkhorn et al., 2012).

Comparing the Locality 22 data to other southern Indian Middle Palaelolithic sites indicates the beginnings of an emerging behavioural pattern. For example, stratified sites in the Kortllayar Basin, Tamil Nadu (Pappu, 2001), and the Lakhmapur area, Karnataka (Petraglia et al., 2003), also show a pattern of raw material movement from hillslope sources out onto floodplain or riverine areas for reduction, as well as the dominant use of a single, locally abundant raw material for the manufacture of a range of artefact types using a variety of reduction strategies. A low percentage of retouched flakes, use of Levallois and discoidal techniques, and local availability of springs and ponded water also characterise these three areas. While the Lakhmapur and Kortallayar Basin Middle Palaeolithic occupations have yet to be dated, the similar activities and geographic habits of the groups living there demonstrate that the Jurreru Valley sequence likely forms part of a wider southern Indian pattern.

Locality 22 provides the bulk of the pre-Toba artefacts used in recent assessments of regional affinity and cultural continuity across the Toba event in southern India (Clarkson et al., 2012; Haslam et al., 2010b), building on previous work on this topic (Petraglia et al., 2007). These analyses demonstrate that the central tendencies of the Jurreru Valley Middle Palaeolithic core technologies cluster tightly with those made by *H. sapiens* from the sub-Saharan African Middle Stone Age, as well as early Southeast Asian and Australian technologies. This apparent technological unity may be the result of an eastwards Late Pleistocene modern human dispersal around the Indian Ocean, beginning some time in MIS 5 (Armitage et al., 2011). Note also that the Locality 22 core central tendencies do not resemble either Neanderthal or early modern human artefacts from Europe, East Africa, Northwest Africa or the Levant, nor do they resemble the European Upper Palaeolithic, the later Indian Microlithic or the earlier Indian Late Acheulean (Clarkson et al., 2012). These results cannot therefore exclude *H. sapiens* as the creators of the pre-Toba Locality 22 assemblage, with the caveat that while core technologies can track regional diversity (Clarkson, 2010), classifications may not reliably map onto biological taxa.

If *H. sapiens* was in southern India prior to 74,000 years ago, the current lack of genetic evidence for such an early presence suggests that they were effectively replaced by later groups of modern humans, supporting a multi-wave model of occupation of India by *H. sapiens* (Keinan et al., 2008; Petraglia et al., 2010; Beyin, 2011; Stringer, 2011). In this scenario, the earliest detectable contributions to the genetic make-up of people living today were made by individuals in the replacement wave. This replacement of early modern humans by the ancestors of living people may have occurred as early as 65,000 years ago according to genetic dating efforts (Macaulay et al., 2005; Kivisild et al., 2006), including attempts to date interbreeding between Neanderthals and the dispersing modern humans (Callaway, 2011). Note that similar

technologies to those found below the tephra at Locality 22 were still present in the Jurreru Valley some 35,000 years after the YTT event (Clarkson et al., 2012), which may indicate either that local cultural traditions were resilient as the new arrivals spread through the region, or that dispersing groups retained Middle Palaeolithic technologies similar to those previously brought to southern India by *H. sapiens*.

If, on the other hand, a different hominin species created the Locality 22 artefacts, the site would provide one of the highest-resolution insights into archaic hominin lifeways in India. It would also represent a surprising technological convergence of archaic Indian stone artefact manufacture with that associated elsewhere around the Indian Ocean with modern humans. This convergence would be of equal interest if archaic groups created the Locality 22 pre-Toba assemblage, and the much later post-Toba artefacts were made by dispersing modern humans. However, as the deposition of much of the post-YTT sediment at Locality 22 likely occurred tens of thousands of years after the eruption, and the site's post-Toba artefact counts are very low, models of continuity or replacement cannot be assessed from this site alone. In the continued absence of skeletal material, recovery of artefacts elsewhere in the Jurreru Valley dated to closely after the eruption would assist in deciding between these alternate scenarios. In this respect, new results emerging from the nearby Locality 3 suggest that contrary to initial reports (Petraglia et al., 2007; Haslam et al., 2010b), dated post-Toba sediments at that site are closer in age to ca. 40 ka rather than the crucial period immediately following the eruption (Balter, 2010; Roberts et al., 2010).

8. Conclusion

Lacunae remain in the understanding of the behavioural and ecological processes underlying Middle Palaeolithic occupation in India, not least of which is that the period continues to be poorly characterised and based on undated, unstratified occurrences. The Jurreru Valley in Andhra Pradesh is proving to be a valuable location for resolving the relationship of palaeoenvironment and demography to technological change in Late Pleistocene India (Petraglia et al., 2007, 2009a; Haslam et al., 2010b). An important component of the Jurreru sequence is the presence of an extensive YTT isochron within a stratified record of Palaeolithic and microlithic occupation, and the Locality 22 site offers the highest-resolution insight into the activities of the valley's inhabitants at the time of the Toba eruption. While Toba likely had less dramatic impacts on global climate and humans than previously hypothesised (especially in southern India), the occurrence of this unambiguous chronological marker will continue to be of great significance in Indian archaeology. Landscapes buried by the tephra may ultimately provide the highest chronological resolution for any Palaeolithic period in South Asia, contributing to ongoing debates over the taxonomic identity and timing of hominin occupation in the subcontinent.

Acknowledgments

Fieldwork and analyses were conducted under permit from the Archaeological Survey of India, with the support of the American Institute of Indian Studies. We thank James Blinkhorn, Venera Espanon, Dorian Fuller, Zenobia Jacobs, Yasaman Jafari, Sacha Jones, Jinu Koshy, Alex Mackay, Christina Neudorf, Oliver Pryce, and Ceri Shipton for technical assistance and comments, and Hari, Mahesh and the villagers of Jwalapuram for assistance in the field. We also thank the two anonymous reviewers for their helpful advice. MP acknowledges major field and laboratory funding from the British Academy and the Leverhulme Trust, MH acknowledges funding for lithic analysis from the McDonald Institute for Archaeological Research, CC acknowledges lithic technology funding from the Australian Research Council, and RGR acknowledges funding from the Australian Research Council for OSL dating and geochemistry. MH is supported by a UK Arts and Humanities Research Council Early Career Fellowship, and CH by an Australian Research Council postgraduate scholarship.

Appendix. Supplementary material

Supplementary data associated with this article can be found, in the online version, at doi:10.1016/j.quaint.2011.08.040.

References

Acharyya, S.K., Basu, P.K., 1993. Toba ash on the Indian subcontinent and its implications for correlation of Late Pleistocene alluvium. Quaternary Research 40, 10–19.
Achyuthan, H., Quade, J., Roe, L., Placzek, C., 2007. Stable isotopic composition of pedogenic carbonates from the eastern margin of the Thar Desert, Rajasthan, India. Quaternary International 162-163, 50–60.
Aitken, M.J., 1998. An Introduction to Optical Dating. Oxford University Press, Oxford.
Andrews, J., Singhvi, A.K., Kailath, A.J., Kuhn, R., Dennis, P., Tandon, S.K., Dhir, R., 1998. Do stable isotope data from calcrete record Late Pleistocene monsoonal climate variation in the Thar Desert of India? Quaternary Research 50, 240–251.
Armitage, S., Jasim, S.A., Marks, A., Parker, A., Usik, V.I., Uerpmann, H.-P., 2011. The southern route "Out of Africa": evidence for an early expansion of modern humans into Arabia. Science 331, 453–456.
Arnold, L., Roberts, R.G., 2009. Stochastic modelling of multi-grain equivalent dose (De) distributions: implications for OSL dating of sediment mixtures. Quaternary Geochronology 4, 204–230.
Balter, M., 2010. Of two minds about Toba's impact. Science 327, 1187–1188.
Beyin, A., 2011. Upper Pleistocene human dispersals out of Africa: a review of the current state of the debate. International Journal of Evolutionary Biology. doi:10.4061/2011/615094.
Blinkhorn, J., Parker, A., Ditchfield, P., Haslam, M., Petraglia, M., 2012. Uncovering a landscape buried by the super-eruption of Toba, 74,000 years ago: a multi-proxy environmental reconstruction of landscape heterogeneity in the Jurreru valley, south India. Quaternary International 258, 135–147.
Blundell, A., Dearing, J., Boyle, J.F., Hannam, J.A., 2007. Controlling factors for the spatial variability of soil magnetic susceptibility across England and Wales. Earth-Science Reviews 95, 158–188.
Callaway, E., 2011. Ancient DNA reveals secrets of human history. Nature 476, 136–137.
Cerling, T.E., 1984. The stable isotopic composition of modern soil carbonate and its relationship to climate. Earth and Planetary Science Letters 71, 229–240.
Chesner, C.A., 1998. Petrogenesis of the Toba Tuffs, Sumatra, Indonesia. Journal of Petrology 39, 397–438.
Chesner, C.A., Luhr, J.F., 2010. A melt inclusion study of the Toba Tuffs, Sumatra, Indonesia. Journal of Volcanology and Geothermal Research 197, 259–278.
Clarkson, C., 2010. Regional diversity within the core technology of the Howiesons Poort techno-complex. In: Lycett, S., Chauhan, P. (Eds.), New Perspectives on Old Stones: Analytical Approaches to Palaeolithic Technologies. Springer, Dordrecht, pp. 43–59.
Clarkson, C., Jones, S., Harris, C., 2012. Continuity and change in the lithic industries of the Jurreru Valley, India, before and and after the Toba eruption. Quaternary International 258, 165–179.
Clarkson, C., Petraglia, M., Korisettar, R., Haslam, M., Boivin, N., Crowther, A., Ditchfield, P., Fuller, D., Miracle, P., Harris, C., Connell, K., James, H., Koshy, J., 2009. The oldest and longest enduring microlithic sequence in India: 35 000 years of modern human occupation and change at the Jwalapuram Locality 9 rockshelter. Antiquity 83, 326–348.
Costa, A., 2011. Were there stone-tipped armatures in the South Asia Middle Paleolithic? Quaternary International, in press.
David, B., Roberts, R.G., Magee, J., Mialanes, J., Turney, C.S.M., Bird, M.I., White, C.D., Fifield, L.K., Tibby, J., 2007. Sediment mixing at Nonda Rock: investigations of stratigraphic integrity at an early archaeological site in northern Australia and implications for the human colonisation of the continent. Journal of Quaternary Science 22, 449–479.
Dearing, J., 1999. Environmental Magnetic Susceptibility. Using the Bartington MS2 System, second ed.. Bartington Instruments Ltd, Oxford.
Dearing, J., Dann, R.J.L., Hay, K., Lees, J.A., Loveland, P.J., Maher, B.A., O'Grady, K., 1996. Frequency-dependent susceptibility measurements of environmental materials. Geophysical Journal International 124, 228–240.
Dennell, R.W., 2007. "Resource-rich, stone-poor": early hominin land use in large river systems of northern India and Pakistan. In: Petraglia, M., Allchin, B. (Eds.), The Evolution and History of Human Populations in South Asia. Springer, Dordrecht, pp. 41–68.

Dennell, R.W., 2009. The Palaeolithic Settlement of Asia. Cambridge University Press, Cambridge.
Eren, M., Durant, A., Neudorf, C., Haslam, M., Shipton, C., Korisettar, R., Petraglia, M., 2010. Experimental examination of animal trampling effects on artifact movement in dry and water saturated substrates: a test case from south India. Journal of Archaeological Science 37, 3010–3021.
Galbraith, R., Roberts, R.G., Laslett, G., Yoshida, H., Olley, J., 1999. Optical dating of single and multiple grains of quartz from Jinmium rock shelter, northern Australia: Part I, experimental design and statistical models. Archaeometry 41, 339–364.
Haslam, M., Clarkson, C., Petraglia, M., Korisettar, R., Bora, J., Boivin, N., Ditchfield, P., Jones, S., Mackay, A., 2010a. Indian lithic technology prior to the 74,000 BP Toba super-eruption: searching for an early modern human signature. In: Boyle, K., Gamble, C., Bar-Yosef, O. (Eds.), The Upper Palaeolithic Revolution in Global Perspective: Essays in Honour of Paul Mellars. McDonald Institute for Archaeological Research, Cambridge, pp. 73–84.
Haslam, M., Clarkson, C., Petraglia, M., Korisettar, R., Jones, S., Shipton, C., Ditchfield, P., Ambrose, S.H., 2010b. The 74,000 BP Toba super-eruption and southern Indian hominins: archaeology, lithic technology and environments at Jwalapuram Locality 3. Journal of Archaeological Science 37, 3370–3384.
Haslam, M., Harris, C., Pal, J.N., Shipton, C., Crowther, A., Koshy, J., Bora, J., Price, K., Dubey, A.K., Clarkson, C., Petraglia, M., 2012. Dhaba: an initial report on an Acheulean, Middle Palaeolithic and microlithic locality in the Middle Son Valley, north-central India. Quaternary International 258, 191–199.
Haslam, M., Korisettar, R., Petraglia, M., Smith, T., Shipton, C., Ditchfield, P., 2010c. In Foote's steps: the history, significance and recent archaeological investigation of the Billa Surgam caves in southern India. South Asian Studies 26, 1–19.
Haslam, M., Petraglia, M., 2010. Comment on 'Environmental impact of the 73 ka Toba super-eruption in South Asia', by M. Williams et al. Palaeogeography, Palaeoclimatology, Palaeoecology 284 (2009), 295–314. Palaeogeography Palaeoclimatology Palaeoecology 296, 199-203.
Haslam, M., Roberts, R.G., Shipton, C., Pal, J.N., Fenwick, J., Ditchfield, P., Boivin, N., Dubey, A.K., Gupta, M.C., Petraglia, M., 2011. Late Acheulean hominins at the Marine Isotope Stage 6/5e transition in north-central India. Quaternary Research 75, 670–682.
Huntley, D.J., Godfrey-Smith, D.I., Thewalt, M., 1985. Optical dating of sediments. Nature 313, 105–107.
Jacobs, Z., Roberts, R.G., 2007. Advances in optically stimulated luminescence dating of individual grains of quartz from archeological deposits. Evolutionary Anthropology 16, 210–223.
Jacobs, Z., Roberts, R.G., Galbraith, R., Deacon, H.J., Grun, R., Mackay, A., Mitchell, P., Vogelsang, R., Wadley, L., 2008a. Ages for the Middle Stone Age of southern Africa: implications for human behavior and dispersal. Science 322, 733–735.
Jacobs, Z., Wintle, A.G., Duller, G.A.T., Roberts, R.G., Wadley, L., 2008b. New ages for the post-Howiesons Poort, late and final Middle stone age at Sibudu, South Africa. Journal of Archaeological Science 35, 1790–1807.
Jacobs, Z., Wintle, A.G., Roberts, R.G., Duller, G.A.T., 2008c. Equivalent dose distributions from single grains of quartz at Sibudu, South Africa: context, causes and consequences for optical dating of archaeological deposits. Journal of Archaeological Science 35, 1808–1820.
Jones, S., 2007. The Toba supervolcanic eruption: tephra-fall deposits in India and palaeoanthropological implications. In: Petraglia, M., Allchin, B. (Eds.), The Evolution and History of Human Populations in South Asia. Springer, New York, pp. 173–200.
Jones, S., 2010. Palaeoenvironmental response to the ~74 ka Toba ash-fall in the Jurreru and Middle Son valleys in southern and north-central India. Quaternary Research 73, 336–350.
Jones, S., Pal, J.N., 2005. The Middle Son valley and the Toba supervolcanic eruption of 74 kyr BP: Youngest Toba Tuff deposits and Palaeolithic associations. Journal of Interdisciplinary Studies in Historical Archaeology 2, 47–62.
Keinan, A., Mullikin, J., Patterson, N., Reich, D., 2008. Accelerated genetic drift on chromosome X during the human dispersal out of Africa. Nature Genetics 41, 66–70.
Kivisild, T., Shen, P., Wall, D., Do, B., Sung, R., Davis, K., Passarino, G., Underhill, P., Scharfe, C., Torroni, A., Scozzari, R., Modiano, D., Coppa, A., de Knijff, P., Feldman, M., Cavalli-Sforza, L., Oefner, P., 2006. The role of selection in the evolution of human mitochondrial genomes. Genetics 172, 373–387.
Kourampas, N., Simpson, I., Perera, N., Deraniyagala, S.U., Wijeyapala, W., 2009. Rockshelter sedimentation in a dynamic tropical landscape: late Pleistocene–Early Holocene archaeological deposits in Kitulgala Beli-lena, southwestern Sri Lanka. Geoarchaeology 24, 677–714.
Kuhn, S., 1990. A geometric index of reduction for unifacial stone tools. Journal of Archaeological Science 17, 583–593.
Macaulay, V., Hill, C., Achilli, A., Rengo, C., Clarke, D., Scozzari, R., Cruciani, F., Taha, A., Shaari, N.K., Raja, J.M., Ismail, P., Zainuddin, Z., Goodwin, W., Bulbeck, D., Bandelt, H.-J., Oppenheimer, S., Torroni, A., Richards, M., 2005. Single, rapid coastal settlement of Asia revealed by analysis of complete mitochondrial genomes. Science 308, 1034–1036.
Maher, B.A., Thompson, R., 1995. Paleorainfall reconstructions from pedogenic magnetic susceptibility variations in the Chinese loess and paleosols. Quaternary Research 44, 383–391.
Mariotti, A., Peterschmitt, E., 1994. Forest savanna ecotone dynamics in India as revealed by carbon isotope ratios of soil organic matter. Oecologia 97, 475–480.
Marwick, B., 2005. Element concentrations and magnetic susceptibility of anthrosols: indicators of prehistoric human occupation in the inland Pilbara, Western Australia. Journal of Archaeological Science 32, 1357–1368.
Matthews, N., Smith, V., Costa, A., Durant, A., Pyle, D., Pearce, N., 2012. Ultra-distal tephra deposits from super-eruptions: examples from Toba and New Zealand. Quaternary International 258, 54–79.
Mellars, P., 2006. Going East: new genetic and archaeological perspectives on the modern human colonization of Eurasia. Science 313, 796–800.
Mishra, S., 1995. Chronology of the Indian Stone Age: the impact of recent absolute and relative dating attempts. Man and Environment 20, 11–16.
Misra, V.N., 1989. Stone Age India: an ecological perspective. Man and Environment 14, 17–64.
Nathan, R., Mauz, B., 2008. On the dose-rate estimate of carbonate-rich sediments for trapped charge dating. Radiation Measurements 43, 14–25.
Oppenheimer, C., 2011. Eruptions that Shook the World. Cambridge University Press, Cambridge.
Oppenheimer, S., 2009. The great arc of dispersal of modern humans: Africa to Australia. Quaternary International 202, 2–13.
Pal, J.N., 2002. The Middle Palaeolithic culture of South Asia. In: Settar, S., Korisettar, R. (Eds.), Indian Archaeology in Retrospect, vol. 1. Prehistory. Indian Council of Historical Research, New Delhi, pp. 67–83.
Pappu, R.S., 2002. The lower Palaeolithic culture of India. In: Paddayya, K. (Ed.), Recent Studies in Indian Archaeology. Munshiram Manoharlal Publishers, New Delhi, pp. 17–59.
Pappu, S., 2001. Middle Palaeolithic stone tool technology in the Kortallayar Basin, south India. Antiquity 75, 107–117.
Pappu, S., Gunnell, Y., Akhilesh, K., Braucher, R., Taieb, M., Demory, F., Thouveny, N., 2011. Early Pleistocene presence of Acheulian hominins in South India. Science 331, 1596–1599.
Pattan, J.N., Pearce, N., 2009. Bottom water oxygenation history in southeastern Arabian Sea during the past 140 ka: results from redox-sensitive elements. Palaeogeography Palaeoclimatology Palaeoecology 280, 396–405.
Perera, N., 2010. Prehistoric Sri Lanka: Late Pleistocene Rockshelters and an Open-air Site. Archaeopress, Oxford.
Perera, N., Kourampas, N., Simpson, I., Deraniyagala, S.U., Bulbeck, D., Kamminga, J., Perera, J., Fuller, D., Szabo, K., Oliviera, N., 2011. People of the ancient rainforest: late Pleistocene foragers at the Batadomba-lena rockshelter. Sri Lanka. Journal of Human Evolution. doi:10.1016/j.jhevol.2011.04.001.
Petraglia, M., 1998. The lower Palaeolithic of India and its bearing on the Asian record. In: Petraglia, M., Korisettar, R. (Eds.), Early Human Behaviour in Global Context. Routledge, New York, pp. 343–390.
Petraglia, M., 2006. The Indian Acheulian in global perspective. In: Goren-Inbar, N., Sharon, G. (Eds.), Axe Age: Acheulian Tool-making from Quarry to Discard. Equinox Publishing, London, pp. 389–414.
Petraglia, M., Clarkson, C., Boivin, N., Haslam, M., Korisettar, R., Chaubey, G., Ditchfield, P., Fuller, D., James, H., Jones, S., Kivisild, T., Koshy, J., Lahr, M.M., Metspalu, M., Roberts, R., Arnold, L., 2009a. Population increase and environmental deterioration correspond with microlithic innovations in South Asia ca. 35,000 years ago. Proceedings, National Academy of Science, U.S.A 106, 12261–12266.
Petraglia, M., Ditchfield, P., Jones, S., Korisettar, R., Pal, J.N., 2012. The Toba volcanic super-eruption, environmental change, and hominin occupation history in India over the last 140,000 years. Quaternary International 258, 119–134.
Petraglia, M., Haslam, M., Fuller, D., Boivin, N., Clarkson, C., 2010. Out of Africa: new hypotheses and evidence for the dispersal of *Homo sapiens* along the Indian Ocean rim. Annals in Human Biology 37, 288–311.
Petraglia, M., Korisettar, R., Bai, M.K., Boivin, N., Janardhana, B., Clarkson, C., Cunningham, K., Ditchfield, P., Fuller, D., Hampson, J., Haslam, M., Jones, S., Koshy, J., Miracle, P., Oppenheimer, C., Roberts, R., White, K., 2009b. Human occupation, adaptation and behavioral change in the Pleistocene and Holocene of south India: recent investigations in the Kurnool district, Andhra Pradesh. Eurasian Prehistory 6, 119–166.
Petraglia, M., Korisettar, R., Boivin, N., Clarkson, C., Ditchfield, P., Jones, S., Koshy, J., Lahr, M.M., Oppenheimer, C., Pyle, D., Roberts, R., Schwenninger, J.-L., Arnold, L., White, K., 2007. Middle Palaeolithic assemblages from the Indian subcontinent before and after the Toba super-eruption. Science 317, 114–116.
Petraglia, M., Schuldenrein, J., Korisettar, R., 2003. Landscapes, activity and the Acheulean to Middle Palaeolithic transition in the Kaladgi basin, India. Eurasian Prehistory 1, 3–24.
Rajagopalan, G., Sukumar, R., Ramesh, R., Pant, R.K., Rajagopalan, G., 1997. Late Quaternary vegetational and climatic changes from tropical peats in southern India - an extended record up to 40,000 years BP. Current Science 73, 60–63.
Rampino, M., Ambrose, S.H., 2000. Volcanic winter in the Garden of Eden: the Toba supereruption and the late Pleistocene human population crash. In: McCoy, F.W., Heiken, G. (Eds.), Volcanic Hazards and Disasters in Human Antiquity. Geological Society of America Special Paper, Boulder, pp. 71–82.
Rampino, M., Self, S., 1992. Volcanic winter and accelerated glaciation following the Toba super-eruption. Nature 359, 50–52.
Rampino, M., Self, S., 1993. Climate-volcanism feedback and the Toba eruption of ~74,000 years ago. Quaternary Research 40, 269–280.
Roberts, R.G., Galbraith, R., Yoshida, H., Laslett, G., Olley, J., 2000. Distinguishing dose populations in sediment mixtures: a test of single grain optical dating procedures using mixtures of laboratory-dosed quartz. Radiation Measurements 32, 459–465.

Roberts, R.G., Jacobs, Z., Fenwick, J., Jafari, Y., Arnold, L., Neudorf, C., 2010. Numerical dating of sediments associated with volcanic ash and stone artefacts in S and NE India. Paper presented at 'The Toba Super-Eruption: A critical moment in human evolution?' conference, Oxford, United Kingdom.

Robock, A., Ammann, C., Oman, L., Shindell, D., Levis, S., Stenchikov, G., 2009. Did the Toba volcanic eruption of ~74 ka B.P. produce widespread glaciation? Journal of Geophysical Research 114, D10107.

Sankalia, H.D., 1964. Middle stone age culture in India and Pakistan. Science 146, 365–375.

Settar, S., Korisettar, R., 2002. Indian Archaeology in Retrospect, vol. 1. Prehistory. Indian Council of Historical Research, New Delhi.

Shea, J.J., Sisk, M., 2010. Complex projectile technology and *Homo sapiens* dispersal into Western Eurasia. PaleoAnthropology 2010, 100–122.

Shipton, C., Bora, J., Koshy, J., Petraglia, M., Haslam, M., Korisettar, R., 2010. Systematic transect survey of the Jurreru valley, Kurnool district, Andhra Pradesh. Man and Environment 35, 24–36.

Sikes, N.E., Potts, R., Behrensmeyer, A.K., 1999. Early Pleistocene habitat in Member 1 Olorgesailie based on paleosol stable isotopes. Journal of Human Evolution 37, 721–746.

Smith, V., Pearce, N., Matthews, N., Westgate, J., Petraglia, M., Haslam, M., Lane, C.S., Korisettar, R., Pal, J.N., 2011. Geochemical fingerprinting the widespread Toba tephra using biotite compositions. Quaternary International 258, 97–104.

Stringer, C., 2011. The Origin of Our Species. Allen Lane, London.

Sukumar, R., Suresh, H.S., Ramesh, R., 1995. Climate change and Its impact on tropical montane ecosystems in southern India. Journal of Biogeography 22, 533–536.

Turney, C.S.M., Flannery, T., Roberts, R.G., Reid, C., Fifield, L.K., Higham, T., Jacobs, Z., Kemp, N., Colhoun, E., Kalin, R., Ogle, N., 2008. Late-surviving megafauna in Tasmania, Australia, implicate human involvement in their extinction. Proceedings, National Academy of Science, U.S.A. 105, 12150–12153.

Westgate, J., Shane, P., Pearce, N., Perkins, W., Korisettar, R., Chesner, C.A., Williams, M., Acharyya, S.K., 1998. All Toba tephra occurrences across Peninsular India belong to the 75,000 yr B.P. eruption. Quaternary Research 50, 107–112.

Williams, M., Ambrose, S.H., van der Kaars, S., Ruehlemann, C., Chattopadhyaya, U.C., Pal, J.N., Chauhan, P., 2009. Environmental impact of the 73 ka Toba super-eruption in South Asia. Palaeogeography Palaeoclimatology Palaeoecology 284, 295–314.

Williams, M., Ambrose, S.H., van der Kaars, S., Ruehlemann, C., Chattopadhyaya, U.C., Pal, J.N., Chauhan, P., 2010. Reply to the comment on "Environmental impact of the 73 ka Toba super-eruption in South Asia" by M. A. J. Williams, S. H. Ambrose, S. van der Kaars, C. Ruehlemann, U. Chattopadhyaya, J. Pal, P. R. Chauhan. Palaeogeography, Palaeoclimatology, Palaeoecology 284 (2009), 295–314. Palaeogeography Palaeoclimatology Palaeoecology 296, 204-211.

Wilson, C., Davidson, D.A., Cresser, M., 2008. Multi-element soil analysis: an assessment of its potential as an aid to archaeological interpretation. Journal of Archaeological Science 35, 412–424.